Effect of Outrigger Position on Motions and Added Resistance of a Trimaran in Various Sea Conditions

by

Leo Nowruzi

National Centre for Ports and Shipping

Australian Maritime College

Submitted in fulfilment of the requirements for the degree of Doctor of Philosophy

University of Tasmania

April 2020

Declarations

Declaration of Originality

This thesis contains no material that has been accepted for a degree or diploma by the university or other institution. To the best of my knowledge and belief, this thesis contains no material previously published or written by another person, except where due acknowledgement is made in the text.

Authority of Access

This thesis may be available for the loan and limited copying and communication in accordance with the Copyright Act 1968.

Signed:

Leo Nowruzi

Date: 17/04/2020

Statement of Published Work Contained in Thesis

The publishers of the papers comprising Chapters 2 and 3 hold the copyright, and for that content, access to the material should be sought from the respective journals. The remaining non-published content of the thesis, and chapter 4 is submitted and are under review, and may be made available for loan and limited copying and communication in accordance with the Copyright Act 1968.

Statement of Co-authorship

The following people and institutions contributed to the publications as part of this thesis:

Leo Nowruzi, Australian Maritime College – University of Tasmania (AMC-UTAS)- (Candidate).

Dr. Hossein Enshaei, AMC-UTAS.

Dr. Jason Lavroff, School of engineering, UTAS.

Prof. Mike R Davis, School of engineering, UTAS.

Dr. Seyedsadreddin Kianejadtejenaki, AMC-UTAS.

Published papers:

1- Nowruzi, L and Enshaei, H and Lavroff, J and Kianejad, SS and Davis, MR, CFD simulation of motion responses of a trimaran in regular head waves, Royal Institution of Naval Architects (RINA) Transactions. Part A1. International Journal of Maritime Engineering, 162, (Part A1) pp. 91-106. ISSN 1479-8751 (2020b).

Located in chapter 2.

Candidate was the primary author while authors 2, 3, 4 and 5 assisted with refinement and presentation. [Candidate: 76%, Author 2: 8%, Author 3: 8%, Author 4: 1%, Author 5: 7%]

2- Nowruzi, L, Enshaei, H, Lavroff J, Kianejad SS, Davis MR. 2020b. Parametric study of seakeeping of a trimaran in regular oblique waves, Ships and Offshore Structures, DOI:10.1080/17445302.2020.1735809.

Located in chapter 3.

Candidate was the primary author while authors 2, 3 and 4 assisted with refinement and presentation. [Candidate: 79%, Author 2: 7%, Author 3: 7%, Author 4: 7%]

3- Nowruzi, L., Enshaei, H., Lavroff, J., Kianejad, S. S. & Davis, M. R. Motions and added resistance of a high-speed trimaran in regular oblique waves. Conference Proceedings, International Conference on Ships and Offshore Structures, ICSOS 2019, Florida, USA, November 4-8 2019 Florida, USA.

Located in chapter 3.

Candidate was the primary author while authors 2, 3, 4 and 5 assisted with refinement and presentation. [Candidate: 82%, Author 2: 6%, Author 3: 5%, Author 4: 1%, Author 5: 5%]

Under review papers:

4- Nowruzi, L., Enshaei, H., Lavroff, J. & Davis, M. R. Effect of speed on motions and added resistance of a trimaran in regular oblique waves, Journal of Ocean Engineering, (Under Review).

Located in chapter 4.

Candidate was the primary author while authors 2, 3 and 4 assisted with refinement and presentation. [Candidate: 84%, Author 2: 6%, Author 3: 5%, Author 5: 5%]

We the undersigned agree with the above stated "proportion of work undertaken" for each of the above published (or submitted) peer-reviewed manuscripts contributing to this thesis:

Signed:

Leo Nowruzi Candidate National Centre for Ports and Shipping, Australian Maritime College University of Tasmania	**Dr Hossein Enshaei** Primary Supervisor National Centre for Ports and Shipping University of Tasmania	**Dr Prashant Bhaskar** Director, National Centre for Ports & Shipping Australian Maritime College University of Tasmania FOR: Mr Michael van Balen AO Principal Australian Maritime College University of Tasmania
Date: 27/04/2020	Date: 27/04/2020	Date: 27/04/2020

Acknowledgement

In the name of God, the most gracious, the most merciful

This research was undertaken with the support of the University of Tasmania and Australian Maritime College. I express my profound gratitude to the University of Tasmania for providing this opportunity for me to evolve to a better version of myself. I also want to say thank you to the staff of the Australian Maritime College Ship Hydrodynamic Centre, Model test Basin and the facility manager, Associate Professor Gregor McFarlane for their input and cooperation.

I would like to express my special thanks of gratitude to my supervising team Dr Hossein Enshaei and Dr Jason Lavroff as well as my technical advisor Professor Michael Davis who gave me the golden opportunity to do this wonderful thesis, which also helped me in doing a lot of research and I came to know about so many new things I am really thankful to them. I thank Dr Nagi Abdussamie for his sincere guidance in my research.

I thank God for the life I'm given to live and for lovers and beloveds. I thank my family, my brother Mohsen who helped me a lot in finalizing this project within the limited time frame, my parents who raised me and have always made me feel special and my sisters, brother in law and niece who have filled my life with love and passion, especially during the last four years.

Finally, I thank God for my failures. I never feel like a failure just because something I tried has failed.

Abstract

Trimaran hull forms provide the ship with larger deck areas and allow for arranging more weights on the upper deck. Also, high slenderness ratio of the centre hull makes it more efficient in reducing the required power. Based on the excessive dependence of trimaran vessels on the position of outriggers, and in order to improve the passenger comfort, it is imperative that the outriggers be carefully spaced near the main hull in order to increase dynamic stability and at the same time, not to increase added resistance of the vessel. Operational circumstances such as wave conditions and operating speed have great impacts on the seakeeping of trimaran vessels. Therefore, many researchers have investigated the resistance of trimarans and some have focused on developing numerical methods for assessing their dynamic performance. Linear Strip theory-based methods have not proven reliable among shipbuilders due to lack of accessibility and comprehensiveness. For instance, linear strip theory-based methods are not reliable when it comes to solving problems considering free surface viscous flows, breaking waves and high speeds. Disadvantages of the current predictive methods as well as limited available experimental data on trimaran motions were the driving forces behind carrying out a computational and experimental study of trimaran behaviour in different sea conditions**.** As a result, a Finite Volume based CFD software, STAR CCM+, is used to solve Reynolds Averaged Navier Stokes (RANS) equations for trimaran motions in various operational speeds and wave conditions. Variations of gridding systems and time steps are investigated, and reliability analysis was performed in solving the RANS equations to improve the accuracy of the results. Moreover, different turbulence models were investigated, and the SST Menter K ω turbulence model proved a more accurate model than Realizable K-ε model. The outcomes were validated against experimental results, which were obtained from a 1.6 m trimaran model tested in various conditions. The tests were carried out in Australian Maritime College Model Test Basin. The impact of transverse, longitudinal and vertical position of outriggers as well as wave interference between the three bodies on the motion response amplitude of the trimaran was investigated.

Comparing the results against secondary data, the CFD model was primarily proved as an effective and reliable method to predict the motions of a trimaran in regular head waves. Then, it was further improved to create the capability of analysing the motions and added resistance of a trimaran in oblique waves. The results suggest that unlike strip theory, the effect of breaking waves, hull shape above waterline and green seas are among those considered in CFD application. Wave deformation as a result of wave-current-wind interaction in CFD was identified as the main source of discrepancy.

Considering the complex wave system between the main hull and outriggers, it was found that the position of outriggers and the hull shape above waterline have significant impact on dynamic performance of the model. With an increase in Stagger ratio (*ST,* longitudinal spacing of main and demi hulls transoms/overall length (x/L)), Separation ratio (*CL*, separation of outrigger centre lines/overall length) and Buoyancy fraction of outriggers (*B, % with respect to centre hull*), the roll motion is reduced, heave motion and added resistance are increased, and pitch motions are slightly influenced. The transverse position of outriggers caused 37% variation in roll peak amplitude, and it was found that the longitudinal position of outriggers can reduce the roll motions

peak amplitude by 80%. The motion behaviour of trimaran hull appeared unique in terms of RAO, where two peaks were identified in roll and heave motions. This is mainly due to trimaran geometry and the effect of reflected waves between the hulls. It was noticed that heave motions and added resistance vary considerably with different outriggers arrangements. The added resistance peak is maximized in configurations leading to minimum roll motion peak amplitudes.

Overall, CFD overestimates the roll responses and underestimates the pitch responses and resistance forces. CFD methods appear to deliver reliable results in predicting both motions and added resistance of trimarans whilst showing similar trends recorded by experimental test in MTB. The maximum discrepancy is 10%-14% in frequency range, where maximum responses occur. The findings further highlight the importance of investigating the impact of operational conditions and outriggers' configurations on the trimaran's dynamic performance as well as the effect of wave interference when undergoing different oblique wave encounter scenarios. The proposed CFD model can be utilised to better understand the wave interference between three bodies of the trimaran. The results of this thesis form the basis for further analysis to investigate other parameters such as extended wave conditions and speeds, size of the outriggers and the weight distribution. This could help establish a more systematic basis for effective design and operation of trimaran vessels in the future.

Table of Contents

List of Figures

List of Tables

Nomenclature

ST	Stagger Ratio (longitudinal position of the outriggers/ hull length) with respect to transom	A_0	Wave amplitude (m)
r	Longitudinal distance between main hull transom and the outrigger transoms (m)	A_3	Heave amplitude (m)
CL	Clearance Ratio (transverse position of the outriggers/ hull length)	A_5	Pitch amplitude (radians)
s	Hull spacing (distance between centre lines of outriggers and main hull) (m)	T_θ	Roll Natural Period (sec)
B_1	Beam of main hull (m)	h	Length of the Cable in Bifilar tests (m)
B_2	Beam of outrigger (m)	X_R	half-length between two supporting cables (m)
B	Waterline Beam overall (m)	ω^*_e	Dimensionless wave encounter frequency ($2\pi\omega_e\sqrt{(L/g)}$, where ω_e is the wave encounter frequency)
Δ	Displacement (kg)	H	Wave Height (m)
Δ_s	Displacement of the outriggers (Kg)	T^*	Pitch Oscillation period (sec)
∇	Volume of displacement (m3)	μ	Wave heading (degrees)
KM	The vertical distance between Metacentre point and Keel (m)	U_I	Uncertainty in iterative convergence
KG	Vertical Position of the Centre of Gravity (VCG) (m)	U_G	Grid spacing uncertainty
GM	Metacentric Height (m)	U_T	Time step uncertainty
KB	The vertical distance between centre of Buoyancy and Keel (m)	R_G	Numerical convergence ratio
BM	The vertical distance between centre of Buoyancy and Metacentre point (m)	U_{GC}	Uncertainty
C_M	Maximum section coefficient	δ^*_{SN}	Numerical error
C_B	Block coefficient	r_G	Grid spacing refinement ratio
C_P	Prismatic coefficient	r_T	Time step refinement ratio
C_{WP}	Waterplane area coefficient	P_G	Order of accuracy
L	Centre hull Waterline Length (m)	$\delta^*_{RE_{G1}}$	Numerical error given by generalised Richardson extrapolation
L_1	Centre hull length (m)	C_G	Correction factor
L_2	Outrigger length (m)	S_3	Variation of simulation results for coarse mesh
V	Forward velocity (m/sec)	S_2	Variation of simulation results for medium mesh
Δ_s	Displacement of the outriggers (kg)	S_1	Variation of simulation results for fine mesh
ρ	Density	TF_3	Heave Transfer Function
T_t	Reynolds Stress Tensor	TF_5	Pitch Transfer Function
μ_t	Turbulent Viscosity	T	CFD calculation time
K	Turbulent Kinetic energy (m^2/sec^2)	C_μ	Realizable time scale coefficient
I	Moment of Inertia (Kg.m2)		
I_x	transverse moment of inertia (Kg.m2)	Fr	Froude number
λ_x	added mass moment of inertia in the roll (Kg.m2)	LCG	Longitudinal Centre of Gravity
m	Mass of the hull (kg)	VCG	Vertical Centre of Gravity
M	Tensor of moments of Inertia (Kg.m2)	$RoG\ roll$	Radius of Gyration for Roll
k	Kinetic Turbulent Energy	$RoG\ pitch$	Radius of Gyration for pitch
C_μ	realizable time scale coefficient	g	acceleration due to gravity
T_v	Viscous Stress Tensor	T_t	Reynolds Stress Tensor

ε	Turbulent Dissipation rate	Δt	CFD time step
ω	Dissipation rate	d	The depth of the basin
ρ	Density	K_v	Wave vector

List of Abbreviation

WIG	Wing in Ground Effect	HYDROS	Doctors Linear Strip Theory based method
RINA	Royal Institution of Naval Architects	AME CRC	Australian Maritime Engineering Cooperative Research Centre
RANS	Reynolds Averaged Navier Stokes	DFBI	Dynamic Fluid Body Interaction
CFD	Computational Fluid Dynamics	VoF	Volume of Fluid
EFD	Experimental Fluid Dynamics	ITTC	International Towing Tank Conference
AMC	Australian Maritime College	RSM	Reynolds Stress Models
MTB	Model Test Basin	DES	Detached Eddy Simulation
TT	Towing Tank	RAO	Response Amplitude Operator
WP_n	Wave Probes		

Chapter 1: Introduction

1.1 Background

The operation of high-speed craft in a high sea-state can produce significantly large motions. These undesirable motions can cause instability as well as passenger discomfort. Nowadays, the trend towards larger high-speed comfortable and stable vessels, in conjunction with widely available modern production technologies, has led to an increasing market for high-speed vessels. These vessels are of growing interest to both naval and commercial shipbuilders due to being fuel-efficient with the reduced travel times. This makes these types of vessels highly desirable to both ship owners and passengers as a result of a quick turn around time. High-speed modern hull forms include but are not limited to hydrofoil supported vessels, multihulls such as catamarans, trimarans and pentamarans, planing crafts, SWATHs, Hovercrafts and Wing in Ground Effect (WIG) vehicles.

Of particular interest to this research are Trimarans, a concept which is based on a ship with a slender main hull supported by two slender outriggers designed to provide the necessary stability to pass various stability criteria. The main hull has low wave making resistance, the major part of a ship's resistance at high speed, and two carefully spaced outriggers restore the stability sacrificed due to the slenderness of the main hull. The main hull and outriggers are then joined together by a cross-structure, which may consist of one or more internal decks depending on the size of the vessel. Thus, the configuration has considerable upper deck space, which allows for the transport of vehicles such as cars and trucks.

The advantages of trimarans over monohulls and catamarans, has been reflected in several published research papers such as Smith and Jones (2001), Lindstrom et al. (1995), Armstrong and Holden (2003), Boote et al. (2004) and Fach (2004), Moolman (2005). These advantages include lower resistance at higher speeds, better damage stability, larger deck area, efficient layout of payload, good stability and reduced operating costs (Bertram and Seif, 2004).

In 1994, the hydrodynamics department of QinetiQ Haslar tested the first frigate trimaran model (Grafton, 2007). Austal, one of the leading shipbuilders of high-speed vessels, has delivered multiple trimaran ships in the past few decades. Figure 1.1 shows two of Austal trimarans, which were designed and built for the Spanish Ferry operator, Fred Olsen for service in Canary Islands and the US navy (Austal-Ships, 2019).

(a)

(b)

Figure 1.1 Trimarans delivered by Austal Ships: (a) "Benchijigua Express", the 127m high-speed vehicle, passenger trimaran ferry, (b) LCS-2 "USS Independence", Littoral Combat Ship trimaran, U.S. Navy. (Austal ships, 2019)

At smaller scale, the 21 m trimaran yacht 'Ilan Voyager' (Figure 1.2a), was built in 1988, and made a record-breaking un-refuelled voyage around Britain in 72 hours. The success of this prototype led to the design and construction of a 35m yacht 'Cable & Wireless Adventurer' (Figure 1.2b). In 2008, Earthrace (later renamed Ady Gil), the biodiesel powered wave-piercing 24 m trimaran (Figure 1.3) set a new world record after completing a circumnavigation in less than 60 days. Later, its newer version, Earthrace 2, was built in 2017. Another example from the naval shipbuilding industry is the French company *CMN Group* that constructed a 43 m patrol trimaran in 2016 (Figure 1.4) which was able to travel 440 km at the speed of 15 knots.

(a)

(b)

Figure 1.2 21 m Ilan voyager (Nigelirens, 1998) (b) Cable & Wireless Adventurer (35 m) (Bluebird Electric, 2014)

Figure 1.3 Earthrace trimaran which broke a world circumnavigation record in 2008 (AdyGil, 2008).

Figure 1.4 43 m French Patrol trimaran which was constructed in 2016 (CMN-Group, 2016).

In vessels such as trimarans, the large upper deck area and the slenderness of the main hull can potentially decrease the dynamic stability of the vessel. This leads to having smaller metacentric height (GM_T), which makes them prone to greater motions when in high seas. Since the outriggers compensate for the loss in GM_T, they need to carefully be spaced near the main hull in order to increase dynamic stability without adversely affecting the resistance. Therefore, the geometrical characteristics of outriggers including their position is of utmost importance. Figure 1.5 shows two circumstances in which a trimaran is having extreme roll motions in calm water.

This chapter aims to provide an explanation of the parameters influencing trimaran roll. Based on the previous research, gaps in research were identified and four main questions are phrased, and accordingly, four objectives were defined. Finally, different methods are utilised to achieve the objectives, and a summary of the methodology and outcomes are given in the last section, namely scope of work.

Figure 1.5 Fred Olsen's Ferry, Benchijigua Express reversing out of Harbour in calm seas showing significant roll (Jersey Action Group, 2016).

1.2 Research and Development

The first trimaran design at the University College London, an Advanced Technology Frigate, was produced by students on the MSc Naval Architecture programme and was presented to the 1992 RINA Affordable Warships Symposium Grafton (2007). Pattison and Zhang (1994) concluded that trimarans have some economic advantages such as reduced wave making resistance, which is the major component of a ship resistance force. Since then, many scholars, Du et al., (2019), Fang and Too (2006), Fang and Chen (2008), Ghadimi et al. (2019), Kim et al. (2019), Wang et al. (2011) and Wu et al. (2011), have investigated the resistance of trimaran vessels both numerically and experimentally. Most of these studies focused on the resistance of trimarans from different aspects. However, a few scholars such as Doctors and Scrace (2004), Yasukawa (2005) and Grafton (2007) switched the focus of their research to motions of trimarans. They mostly used linear and non-linear potential flow-based strip theories for predicting the motions of trimaran vessels. Hebblewhite, Sahoo, & Doctors (2007) constituted a focus on the effect of the longitudinal position of outriggers on the motion characteristics of a trimaran hull form in head seas. Their comparison between the model tests and the strip theory method results was aimed to assess the theoretical capacity of HYDROS (strip theory based) to predict the motion characteristics of a trimaran hull form in head seas. One of the most recent motion studies of trimarans in oblique seas was carried out by Dobashi (2014), where he used a strip theory-based method to predict motions of a trimaran in oblique waves. His method was not validated against experimental data and did not consider hydrodynamic interaction between the main hull and outriggers.

Beck et al. (2001) and Tezdogan et al. (2014a) suggested that the effects of breaking waves, turbulence and viscosity can be taken into account by Reynolds–Averaged Navier–Stokes (RANS) methods. Thus, applications of CFD-based RANS methods are rapidly growing in terms of seakeeping computations Tezdogan et al. (2014b) to improve accuracies in predicting ship motion responses.

1.3 Research Opportunity

According to the literature review, there is a limited range of research data available that focuses on the seakeeping aspects of trimarans regarding the outriggers' configurations. For instance, no available experimental data on the impact of vertical position of outriggers (or outriggers buoyancy fraction of the main hull) on the motions of trimarans were found. There is limited published verified experimental data regarding trimaran motions in oblique seas. Furthermore, existing numerical models do not consider the effect of breaking waves, viscosity and the wave interference between the main hull and outriggers and there is limited access to verified predictive tools for analysing dynamic performance of trimarans in oblique waves.

Most of the prior predictive methodologies are limited in terms of considering the effects of viscosity and turbulence. These effects may increase when there are wave interaction effects between the three bodies of a trimaran. Some of these limitations can be addressed by more advanced theories, such as unsteady methods. Therefore, it is essential that a CFD model is well understood and validated for future studies in predicting the vessel response according to parametric changes.

1.4 Research Questions

The proposed work is broken down into several specific research questions as follows:

- What is the impact of the longitudinal, transverse and vertical position of outriggers on the motion characteristics of a trimaran?

- What is the impact of operational speed and the wave interference between the main hull and outriggers on the dynamic performance of a trimaran vessel?

- Can Computational Fluid Dynamic (CFD) methods achieve better results than previous software solutions such as linear strip theory methods?

- With the advancement of technology, can CFD methods be used with increased confidence when compared against experimental methods in assessing trimaran motions in oblique sea directions?

1.5 Research Objectives

The following procedures have been undertaken in order to answer the research questions outlined above.

- To develop a validated CFD model in order to calculate the motions of a trimaran in head seas.

- To investigate the impact of transverse, longitudinal and vertical position of outriggers on the motions and added resistance of the trimaran.

- To further develop the CFD model to oblique seas conditions.

- To investigate the impact of operational speed and different wave conditions such as wave height, frequency and direction on the motions response and added resistance of a trimaran.

1.6 Scope of Work

To achieve these objectives, the research intends to particularly focus on the impact of outriggers' configurations on trimarans motions in both head and oblique waves by using a combination of computational (CFD) and experimental techniques. Those techniques are used to analyse the dynamic performance of a trimaran with various outrigger configurations, operational speeds and wave conditions. Also, the results of simulations of a trimaran utilising a Finite Volume based CFD software, STAR CCM+, is validated against experimental test data to provide a verified model for further investigations in the future.

The trimaran model consists of Model 9 of AME CRC systematic series and two scaled down outriggers with a scale factor of 0.459. The hulls were assembled with struts to form a 1.6 m model scale high-speed trimaran. Throughout the study, this model is investigated under different test conditions. The scope of work undertaken in this thesis is summarised as follows:

- Primarily, a CFD based software is used to investigate the dynamic performance of a trimaran at different speeds and in regular head wave conditions. Dynamics of the multi-phase free surface flows and free surface air and water interaction effect on the performance of the trimaran is investigated. The efficiency of the simulation process is studied by investigating the effects of various operating conditions on the motions of a trimaran. Various Turbulence models (SST menter K-ω and Realizable K ε) are studied and reliability analysis for different gridding systems, boundary conditions and time discretization methods are performed. The time series of the heave and pitch motions are analysed in eighteen cases and the transfer functions are obtained for Froude numbers of 0.3 and 0.5 (equivalent speeds of 1.19 and 1.98 m/sec at model scale). The results of an experimental head seas tests, (Hebblewhite, Sahoo, & Doctors, 2007), are used to validate the CFD results. The outcomes are also compared against a Strip Theory-based method (HYDROS), and the main sources of discrepancies are discussed (Chapter 2).
- Seakeeping tests in oblique seas are carried out at AMC-MTB. The 35 m long and 12 m wide MTB set up was modified to add the capability of performing tests in oblique seas. More than 500 tests were conducted and the effects of the outrigger configuration on the dynamic performance of a trimaran was investigated. Eight different arrangements of outriggers for the trimaran model were tested at different speeds and a range of wave encounter frequencies. A constant wave heading, and wave height were maintained. Three motion components (heave, pitch and roll amplitudes), as well as added resistance of the model are analysed comparatively, and the potential mechanisms behind the variations including the wave interaction between the main hull and outriggers are discussed (Chapter 3).
- Considering the limitation and availability of experimental oblique seas tests in different conditions and for different geometries, the final component of the thesis is to develop the CFD capability to analyse trimaran

motions in various oblique wave conditions. Therefore, the head seas CFD model, which was developed in Chapter 2, was extended to be able to analyse the dynamic performance of the trimaran in oblique waves. The CFD model was then validated against experimental data collected during model scale tests from the AMC MTB. Then, the model is utilised to discuss the mechanism behind motion and added resistance variations of the trimaran in different speeds and wave conditions (Chapter 4).

Chapter 2 has been removed for copyright or proprietary reasons.

It has been published as: Nowruzi, L., Enshaei, H., Lavroff, J., Kianejad, S. S., Davis, M. R., 2019a. CFD simulation of motion responses of a trimaran in regular head waves, Transactions of the Royal Institution of Naval Architects Part A: International journal of maritime engineering, 162(A1), 91-106

Chapter 3 has been removed for copyright or proprietary reasons.

It has been published as: Nowruzi, L., Enshaei, H., Lavroff, J., Davis, M. R., 2020. Parametric study of seakeeping of a trimaran in regular oblique waves. Ships and offshore structures, 15(sup 1), S98-S109,

and as,

Nowruzi, L., Enshaei, H., Lavroff, J., Kianejad, S. S., Davis, M.R., Motions and added resistance of a highspeed trimaran in regular oblique waves, Proceedings of the International Conference on Ships and Offshore Structures, ICSOS 2019, Florida, USA; 2019 November 4-8.

Chapter 4: The effect of speed on the motions and added resistance of the trimaran in Oblique seas: CFD and experimental approach

The works presented in this chapter has been submitted as a peer reviewed paper to the Journal of Ocean Engineering (Under Review).

Abstract

Trimaran hull forms provide the ship with larger deck areas and allow for more weight as cargo and passengers due to the flat upper deck section. This leads to having a smaller metacentric height (GM_T), which may cause this type of hull configuration to be prone to greater roll motions. Computational Fluid Dynamic methods have proven efficient in predicting trimaran motions in head seas by solving unsteady Reynolds–Averaged Navier-Stokes (RANS) equations. However, there are still limited computational and numerical studies that have investigated the dynamic response of such vessels in oblique seas. Since roll motions are of utmost importance in passenger comfort and vessel dynamic stability, it is essential to have a better understanding of the parameters that influence trimaran roll in oblique seas. The research reported in this paper intends to analyse the effect of speed on the motions of a high-speed trimaran in regular oblique seas. The reliability of current CFD methods in modelling complex wave interactions of multihull vessels in a wide range of wave frequencies and speeds has also been investigated. In order to validate the computational data, the motions response and added resistance of the trimaran model were measured in regular oblique seas during experiments undertaken at the Australian Maritime College Model Test Basin. A CFD model was developed using StarCCM+ and the validation of the method is discussed. The results suggest that motion responses and added resistance of the representative trimaran vary considerably with speed variation. Roll and heave responses have an opposite trend and CFD results are in good agreement with model test data for most conditions. The results from this investigation have therefore provided an improved understanding of the seakeeping performance of trimarans in oblique seas that is in particular applicable to both ship design and future operation.
Keywords: trimaran; added resistance; speed variation; heave motions; pitch motions; roll motions; oblique seas.

4.1 Introduction

Trimaran hull forms provide designers with increased flexibility when it comes to the general arrangement of the main deck area design. Different researchers have discussed multiple advantages of these hull types over monohulls and catamarans (Armstrong and Holden, 2003, Boote et al., 2004, Fach, 2004, Lindstrom et al., 1995). Pattison and Zhang (1994) investigated the trimaran performance in waves and calm water. Their investigations later led to building the British research vessel Triton. Wang et al. (2011) investigated the wave-making resistance and transverse stability of high-speed trimarans. Others (Du et al., 2019, Fang and Too, 2006, Ghadimi et al., 2019, Kim et al., 2019, Wang et al., 2018, Wu et al., 2011) have also investigated the trimaran design both numerically and experimentally. However, in terms of motion responses, there is still limited understanding and limited data available for validation in particular for oblique seas test conditions both numerically and experimentally. This confirms the necessity of more investigation of dynamic performance of such vessels (Jersey Action Group, 2016, JT901, 2015).

Faltinsen and Zhao (1991) questioned the validity of existing numerical methods when applied at lower speeds. Doctors and Scrace (2003) investigated the influence of different parameters such as speed and wave conditions on transom flows of trimarans. They concluded that the radiated wave interaction between the hulls at lower speeds can reduce the reliability of the numerical models. However, at higher speeds, the predictions improve due to less wave interaction between the main hull and outriggers. Yasukawa (2005), Grafton (2007) and Dobashi (2014) used both linear and non-linear potential flow-based seakeeping theories for predicting the roll motions of trimaran vessels. Each identified the disadvantages of these methods such as the effect of viscosity, turbulence and transom stern. Onas (2009), used a 6 Degree of Freedom (DOF) potential flow Rankine-panel numerical method to study and validate the impact of the longitudinal and transverse positions of the outriggers on the hydrodynamic coefficients of a prototype trimaran. He was able to investigate the roll response by WASIM CFD software. Hebblewhite, Sahoo, & Doctors (2007) studied the motions of a high-speed trimaran model in head seas and by shifting the outriggers rearward identified experimentally the parameters influencing the heave and pitch response. All studies reported the effect of reflected waves on the accuracy of their models at lower speeds.

Past numerical studies have been limited in terms of considering the effect of viscosity and turbulence. Some of these limitations can be addressed by using unsteady Reynolds Averaged Navier–Stokes (RANS) methods (Beck et al., 2001). Tezdogan et al. (2014a) suggested that as a consequence of advancement in computations, using RANS methods to study seakeeping problems is more reasonable, where the effects of breaking waves, turbulence and viscosity could be taken into account (Simonsen et al., 2013). Thus, application of CFD-based RANS methods is growing in terms of seakeeping prediction (Tezdogan et al., 2014b). The validity of CFD methods in solving RANS equations for calculating the motions of a high-speed trimaran in head seas is also discussed in-detail in Chapter 2. After comparing the results against linear strip theory methods and experimental data, a better result for trimaran motions in head seas was achieved by CFD in comparison to the LST methods.

In this current research investigation, the effect of speed on heave, pitch and roll motion as well as added resistance of a trimaran is studied. The main mechanisms behind the variations are discussed and the data is used to validate the results of a CFD model. Finally, the CFD simulations are further extended to study the effect of waves and green seas over the bow deck on the seakeeping performance of the vessel at different speeds and wave configurations. The main objective of this study is to understand the parameters influencing the motions response of a trimaran model in oblique seas by using CFD for simulation. This aimed at developing a predictive simulation model for investigating motion sensitive parameters in the future. Therefore, Response Amplitude Operators (RAOs) of heave, pitch and roll motions as well as added resistance for Froude numbers of 0.3, 0.4 and 0.5 (equivalent speeds of 1.19, 1.51 and 1.98 m/s at model scale) are obtained and analysed comparatively. Finally, the sources of the discrepancy and the physics of the phenomena are discussed.

4.2 Trimaran Model Experiments

Based on the objectives of the research undertaken, a set of oblique seas experiments were carried out at the Australian Maritime College Model Test Basin. The equipment was calibrated daily and three motion components of a trimaran model in roll, heave and pitch as well as added resistance force were recorded as time histories for different speeds and wave configurations. Figure 4.1 shows a 1.6 metre 16 kg trimaran test model, which has hull forms based on Model 9 of the Australian Maritime Engineering CRC systematic series. A schematic diagram of the model is shown in Figure 4.2, and Table 4.1 summarises the model particulars. Full details about the model and experimental setup are also presented in Chapter 3, Sections 3.2 and 3.3.

Figure 4.1 The trimaran model tested at AMC Model Test Basin (MTB).

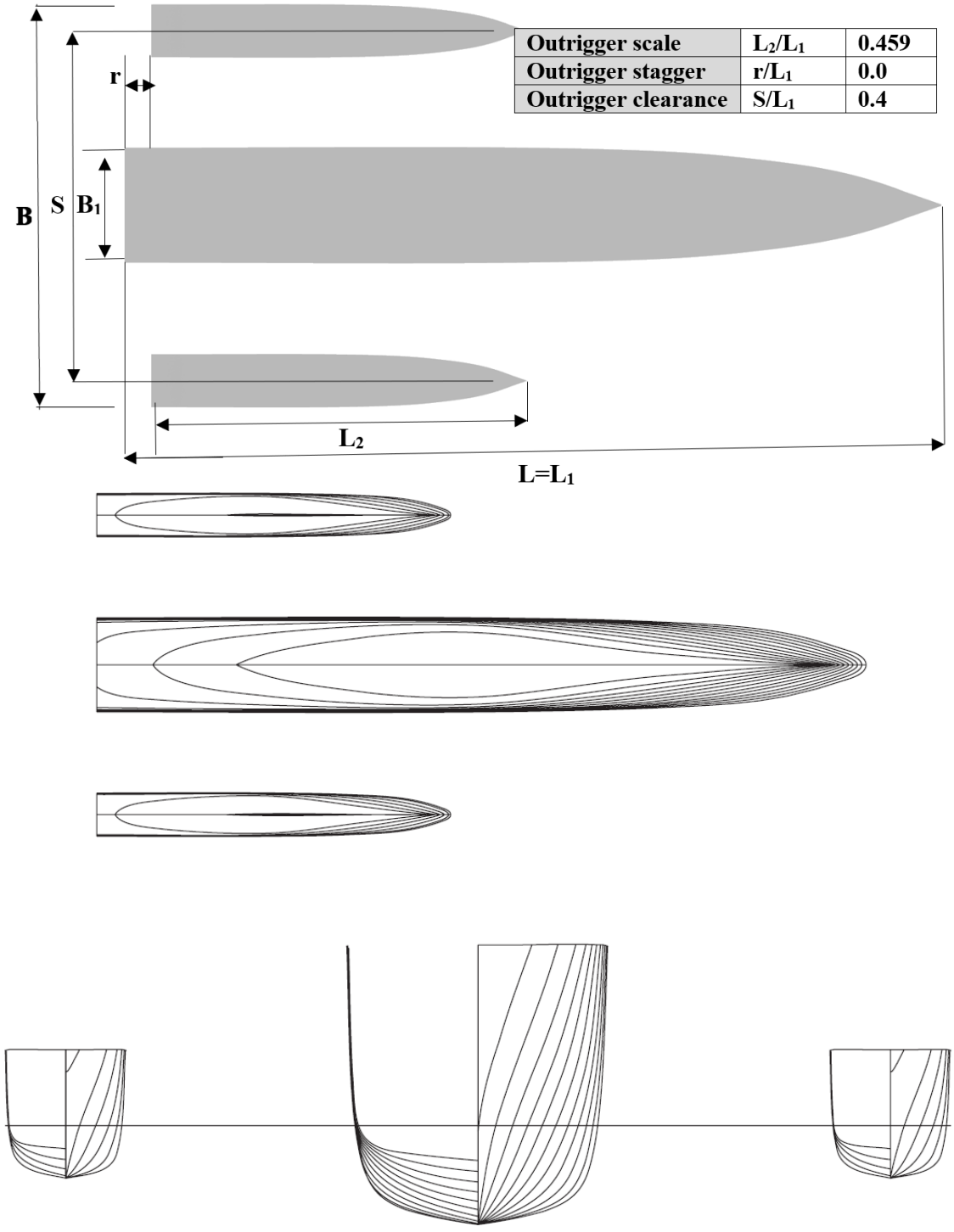

Figure 4.2 Lines and body plan of trimaran model based on Model 9 of the Australian Maritime Engineering CRC systematic series. A 1.6 m 16 kg trimaran model.

As shown in Figure 4.2, Stagger ratio (ST) is defined as r/L1, where r is the distance between the outrigger transoms and the main hull transom, and L1 is the length overall of the main hull. Separation ratio (CL) is defined as S/L1, where S is the distance between outrigger's centre lines. CL is used to describe the ratio for the transverse position of the outriggers.

Table 4.1 Details of the trimaran model 9 of CRC series.

Item	***Symbol***	***Value***

Main hull Displacement mass (kg)	Δ	12.8
Waterline length (m)	L	1.6
Waterline beam (m)	B	0.2
Draft (m)	T	0.08
Waterplane-area coefficient	C_{WP}	0.796
Maximum section coefficient	C_M	0.8
Block coefficient	C_B	0.5
Prismatic coefficient	C_P	0.624
Slenderness coefficient	$L/\nabla^{1/3}$	6.817
Outrigger displacement mass(kg)	Δ_s	3.18
Outriggers scale ratio	L_2/L	0.459
Outriggers stagger ratio	r_2/L	0
Outriggers spacing (separation ratio)	$CL=s/L$	0.4
Vertical Centre of Gravity (m)	VCG	0.091
Roll Radius of Gyration	RoG_{Roll}	0.25
Pitch Radius of Gyration	RoG_{Pitch}	0.4

4.2.1 Measurement of mass properties of the 1.6m trimaran model

In order to have a precise comparison of motion responses between CFD and experiment, it was necessary to take some pre-test measurements. Radius of gyration and the metacentric height have a direct influence on the motions of the vessel; therefore, these parameters were measured directly. Since the static trim was maintained at zero, the Longitudinal Centre of Gravity (LCG) is thus equal to the Longitudinal Centre of Floatation (LCB). Inclining tests were conducted to measure the Vertical Centre of Gravity (VCG). Radius of Gyration in pitch RoG_{Pitch}, was measured using the Bifilar method and Radius of Gyration in roll $RoG_{Roll,}$ was measured by roll oscillation tests. Further details are provided in Section 3.2.

4.2.2 AMC Experimental Test Facilities

The experiments were carried out in Australian Maritime College Model Test Basin (MTB). The truss gantry was arranged in a diagonal direction to run the model at an encounter wave heading of 160.9^o (Figure 4.3). The model was connected to the carriage and was placed at a distance of 26 m from the wave maker, and a wave damping beach with a slope of 9 degrees was located at the same end of the basin as the model starting position. This and the fact that the wave propagation direction was opposite less than the forward speed of the model helped to minimise wave reflection effects.

To monitor the wave height and frequency of encountered waves, three wave probes were used. Two of them were stationary (Wave Probe 1 = WP1, Wave Probe 2 = WP2) and were placed along the side of the basin tank, 0.6 m from the inner tank wall and at a horizontal distance of 4.5 m and 16.5 m from the wave maker respectively (refer to Figure 4.3). The third Wave Probe (WP3) was a moving wave probe which was attached to the carriage at 1.35 metre distance from the model. A wave damping beach with a slope of 9^o was located at the opposite end to the wave maker as shown in Figure 4.3. Each experiment was carried out every 40 minutes to to provide calm water before commencing the next model test wave run.

A Qualisys Manager system with eight cameras was used to capture the motions of the model (Figure 3). The model was constrained in yaw and sway directions. Surge motion was restricted to the carriage speed

and the model was free to heave, pitch and roll. A load cell was used on the forward tow post to measure the resistance force during each test condition, and a wireless system was used to record and transfer load cell and moving wave probe data to a desktop All devices were synchronised, and the capturing data rate was set at 200 Hz for wave probes (static and moving), load cell and the Qualisys motion measurement system.

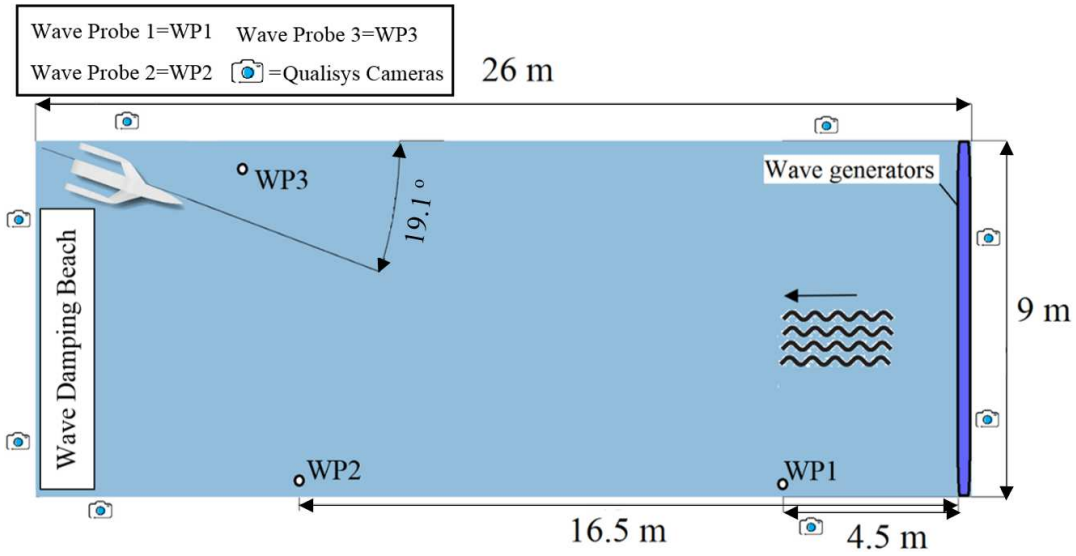

Figure 4.3 Plan view of 1.6m trimaran model test set up at the AMC Model Test Basin.

The carriage speed was set at 1.19 m/s at its lowest setting, and the truss was approximately 27 meters long. Thus, it took at least 22.5 seconds to run each experiment at the lower speed setting. The wave maker was located on the opposite end of the basin, and the generated waves were towards the forward motion of the carriage (Figure 4.3). Further details were provided in Section 3.3.

4.2.3 Experimental Test Conditions

The model tests were carried out at three speeds of 1.19, 1.59 and 1.98 m/s (equivalent Froude numbers of 0.3, 0.4 and 0.5). The wave height and chosen wave heading were 0.06 m and 160.9 respectively. The model was tested at eight dimensionless encounter wave frequencies, ranging from ω_e^* = 1.72 to ω_e^* = 7.42 with increments of about 0.5 (0.1 Hz). In each experiment time traces of heave, pitch and roll as well as resistance were captured. The uncertainty analysis was also performed based on the ISO-GUM method with further details of the uncertainty analysis reported in section 3.4.1.

A sample time series of the trimaran model motions at a forward test speed of 1.19 m/s (Froude Number = 0.3), wave height of 60mm and dimensionless encounter wave frequency of ω_e^* = 4.36 is shown in Figure 4.4.

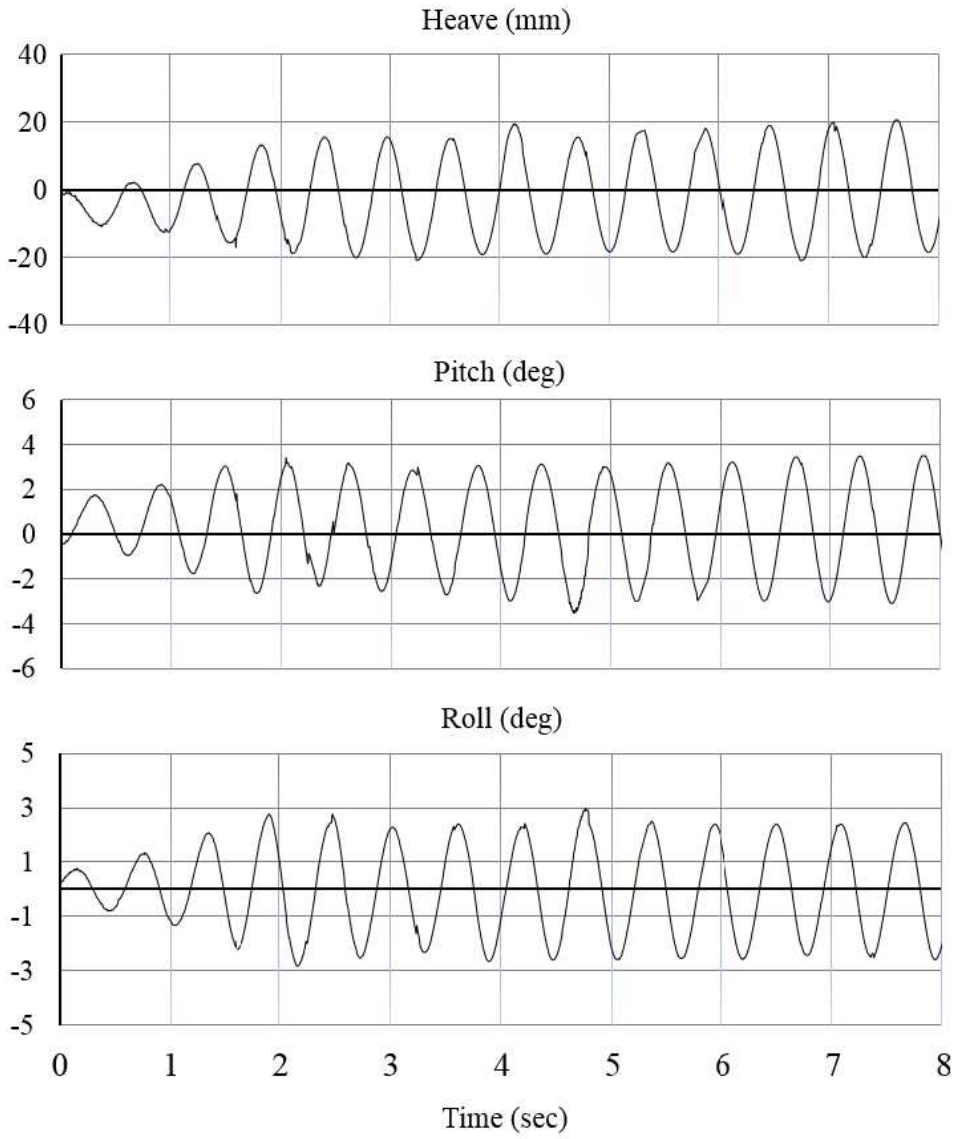

Figure 4.4 Experimental heave, pitch and roll motions of the trimaran model at a model test speed of 1.19 m/s (Froude number = 0.3), dimensionless wave encounter frequency of ω_e=4.36, wave height of 60 mm and wave heading of 160.9º.*

4.2.4 *Forward Speed Effects on Trimaran Model Motions*

The Response Amplitude Operators (RAO) of the trimaran were determined based on the experimental model test results obtained at the Model Test Basin. Figure 4.5 shows the heave, pitch and roll RAOs as well as resistance force obtained at three forward speeds of 1.19, 1.59 and 1.98 m/s (equivalent Froude number of 0.3, 0.4 and 0.5). That is to make sure the entire range of possible speed is captured by the test facility within the MTB. These tests were undertaken at a set wave height of 60 mm and wave heading of 160.9º. As expected, the heave RAO approaches unit value at low frequency and the roll RAO approaches the Sine of the heading (0.325) whilst the pitch RAO is tending towards the Cosine of the heading angle (0.925).

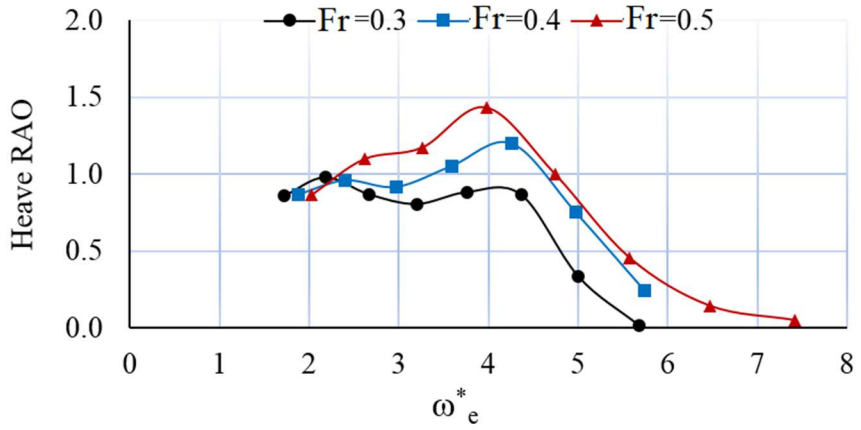
Fr=0.3
Fr=0.4
Fr=0.5
Heave RAO
2.0
1.5
1.0
0.5
0.0
0
1
2
3
4
5
6
7
8
ω*e

(a)

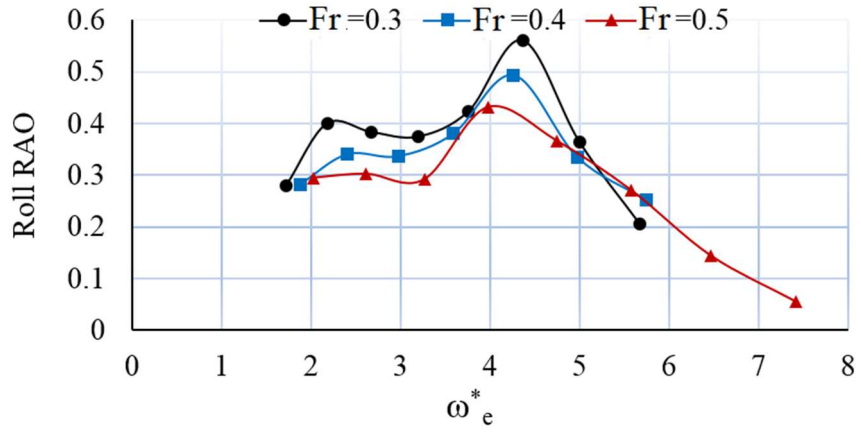
Fr=0.3
Fr=0.4
Fr=0.5
Roll RAO
0.6
0.5
0.4
0.3
0.2
0.1
0
0
1
2
3
4
5
6
7
8
ω*e

(b)

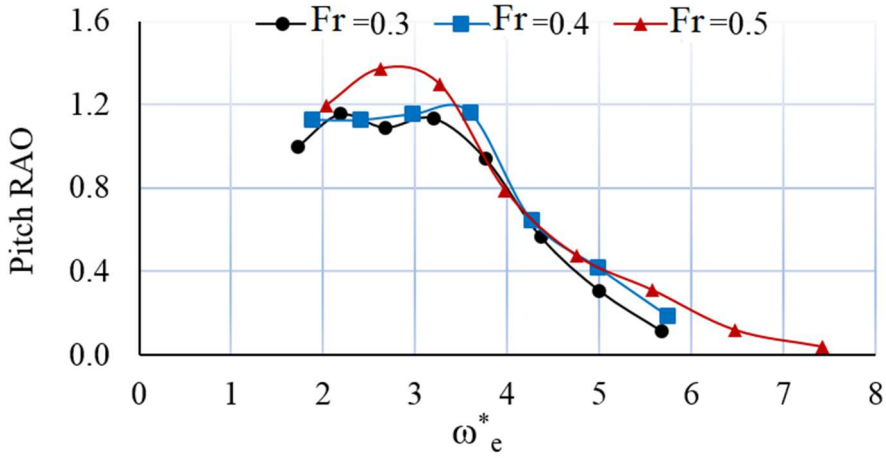
Fr=0.3
Fr=0.4
Fr=0.5
Pitch RAO
1.6
1.2
0.8
0.4
0.0
0
1
2
3
4
5
6
7
8
ω*e

(c)

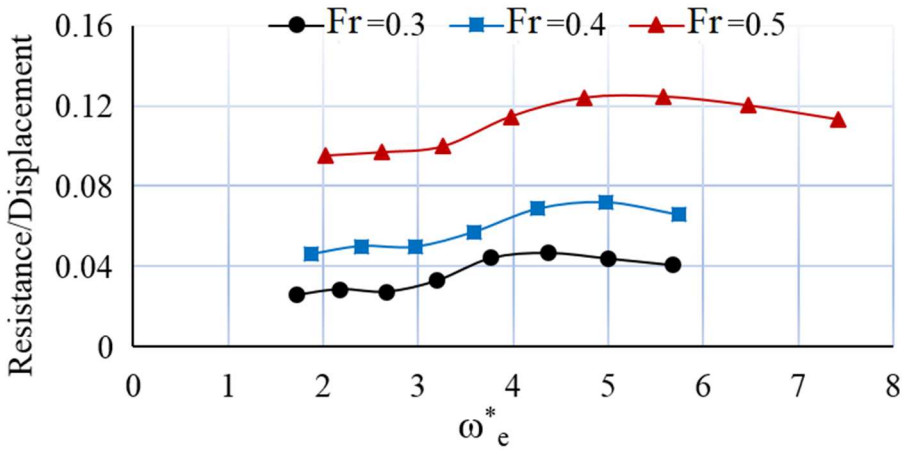

(d)

Figure 4.5 Heave, pitch and roll transfer functions and resistance to displacement ratio of the high-speed trimaran model at speeds of 1.19, 1.59 and 1.98 m/s (Froude numbers of 0.3, 0.4 and 0.5 respectively) at a wave height of 60 mm and wave heading 160.9 °.

The natural roll period, T_θ is estimated as given by Equation (4.1) (Bhattacharyya 1978, Lloyd 1989, Molland 2011):

$$T_\theta = 2\pi K\sqrt{\frac{1}{g*GM}} \tag{4.1}$$

Where K is the roll Radius of Gyration (RoG roll), GM is metacentric height and g is the acceleration due to gravity. Having K and GM measured from experiment, the calculated value and the measured response from oscillation tests for the roll natural period and frequency are compared in Table 4.2.

Table 4.2 Measured and calculated values of natural roll frequency for the trimaran model.

	Measured (sec)	Calculated (s
Roll Natural Period (T_θ)	*0.59*	*0.59*
Dimensionless Natural Roll Frequency	*4.3*	*4.3*

The heave and roll amplitude operators shown in Figures 4.5(a) and 4.5(b), have an opposite trend: with an increase in speed, the roll response decreases, and the heave response increases. It is to be noted that the roll and heave peak responses for all speeds are at a dimensionless wave frequency of about ω_e*=4.3 which is also close to the natural roll frequency for this configuration. Although responses at the peak frequencies occur either at 4 or close to 4 for heave and roll, there are considerable variations observed at different speeds. For the lower frequencies where heave motion is close to 1.0, the response magnitude varies from 0.86 to 1.43 and increasing the operational speed has a notable effect on increasing the heave response as shown in Figure 4.5 (a). In the case of roll motion, where the response magnitude varies between 0.43 to 0.56, increases in forward speed reduced the roll response of the model (Figure 4.5 (b)).

The trends observed for the RAO plots shown in Figure 4.5 appear to follow similar patterns with increasing speed. The RAO responses generally show two peaks to be significant at particular frequencies, and the curves taper off sharply after the second peak at high frequency as expected. The development of these two peaks is mainly due to the wave interaction effects between the main hull and outriggers further discussed in

section 3 below. At Fr=0.5 this effect reduces to just one main peak for the roll and heave response amplitudes, which could be due to less wave interaction effects at high speed as might be expected.

The trend observed in the plots for pitch motions shown in Figure 4.5(c) appears to follow a similar pattern for lower speeds (Fr=0.3 and Fr=0.4), but for Fr=0.5 the local peak is significantly higher and occurs at a lower encounter frequency, ω_e*=2.5. This is mainly due to variation in the wave interaction between the main hull and outriggers at higher speeds. However, the speed sensitivity to pitch response was not as significant as that observed in the roll and heave responses as shown in the RAO plots.

The model speed affects the added resistance magnitude considerably as demonstrated in Figure 4.5(d). The variation seems proportionate to the square of speed (V^2) as would be expected for calculating drag. The magnitude of maximum resistance to displacement ratio for Fr=0.5 is about 0.1244 and reduces to 0.072 and 0.044 at lower Froude numbers of Fr=0.4 and Fr=0.3 respectively. All peaks occur at the dimensionless wave frequency of close to $\omega_e^* = 5$.

4.3 Trimaran Model CFD Simulation in Oblique Seas

Having obtained quantitative experimental data from the trimaran oblique seas model tests, developing a CFD capability as a predictive tool not only assists in extending computational development but also helps understand the parameters influencing the ship motions response. To this end a series of simulations have been carried out using a commercial unsteady RANS solver, STAR-CCM+, and the results are discussed in comparison with the experimental results.

The software uses the mean quantity equation to solve the Reynolds Navier-Stokes equations (CD-Adapco, 2017). The equations for the mean quantities are essentially identical to the original Navier-Stokes equations, except that an additional term known as the Reynolds stress tensor T_t, appears in the momentum transport equation as given by Equation (2):

$$T_t \equiv -\rho\overline{v'v'} = -\rho\begin{pmatrix} \overline{u'u'} & \overline{u'v'} & \overline{u'w'} \\ \overline{u'v'} & \overline{v'v'} & \overline{v'w'} \\ \overline{u'w'} & \overline{v'w'} & \overline{w'w'} \end{pmatrix} \quad (4.2)$$

To solve the problem, the Reynolds stress tensor T_t, of the above equation in terms of the mean flow quantities should be modelled for the closure of the governing equations. Two basic eddy viscosity models (Realizable K-ε and SST Menter K-ω turbulence models) are used. Eddy viscosity models use the concept of a turbulent viscosity μt to model the Reynolds stress tensor as a function of mean flow quantities. These models solve additional transport equations for scalar quantities that enable the turbulent viscosity μt to be derived (CD-Adapco, 2017). For realizable K-ε and SST Menter K- ω turbulence models, the turbulent viscosity is calculated by Equations (4.3) and (4.4), respectively.

$$\mu_t = \rho C_\mu \frac{k^2}{\varepsilon} \quad (4.3)$$

$$\mu_t = \rho k T \quad (4.4)$$

where ρ is the fluid density, k is the turbulent kinetic energy, ε is the turbulent dissipation rate, T is the viscous stress tensor and C_μ is a realizable time scale coefficient. T and C_μ are not constant and are calculated independently. In order to analyse motions of the trimaran, a Dynamic Fluid Body Interaction (DFBI) model was used with the vessel free to move in roll, pitch and heave directions. The DFBI model enabled the RANS solver to calculate the exciting force and moments acting on the trimaran hull due to waves and currents, and to solve the governing equations of rigid body motion in order to re-position the rigid body. A Volume of Fluid (VoF) model was used in a Eulerian frame to simulate flows of a pair of immiscible fluids (air and water) on numerical grids and to resolve the interface between the phases. In order to obtain sharp interfaces between the phases, the 2nd-order discretization scheme is used. VOF waves were used to simulate the regular surface gravity waves on a light fluid (air) - heavy fluid (water) interface. They were used with the Volume of Fluid (VoF) multiphase model with the three degree of freedom motion model. When created, VoF Waves provide field functions that can be used to initialize the VoF calculation and to provide suitable profiles at boundaries. A first order wave is modelled with a first order approximation to the Stokes theory of waves (Table 4.3). The dimensions of the domain fulfil ITTC Procedures (2011), and the equations for the first order wave approximation are as shown in Table 4.3. Where T, λ, a, ω, d, z and K_v are the wave period, wavelength, wave amplitude, wave frequency, the depth of the basin, the vertical distance from the mean water level and wave vector, respectively.

Table 4.3 1st order VoF wave, Stocks wave theory.

Description	Equation
The *horizontal Velocity*	$v_h = A_0\omega\cos(K_v.x - \omega t)\, e^{Kz}$
The *vertical Velocity*	$v_h = A_0\omega\sin(K_v.x - \omega t)\, e^{Kz}$
The *surface elevation*	$\eta = A_0\cos(K_v.x - \omega t)$
The Dispersion relation for 1st order wave in finite water depth	$T = \left[\frac{g}{2\pi\lambda}\tanh\left(\frac{2\pi d}{\lambda}\right)\right]^{-1/2}$

An overset region, which includes the trimaran hull body, moves with the hull (moving mesh) over a fixed background mesh of the domain as shown in Figure 4.6. This saves computational time and allows the generation of a refined mesh system without compromising the accuracy (Field and Wayne, 2013). An automatic surface re-mesher tool is used to retriangulate the surface. The top, bottom, left and right boundaries of the domain can either be defined as wall boundary conditions (to model a virtual towing tank) or velocity inlet. Setting boundaries as a velocity inlet with a parallel velocity component prevents the fluid interaction with boundaries and avoids development of a velocity gradient between the fluid and the wall (Date and Turnock, 1999). The velocity for the above-mentioned boundaries and the inlet boundary were set to the velocity of the trimaran tested in the Model Test Basin.

The final grid size in the free surface and around the hull is about 1 millimetre, which is 30 times smaller than the wave amplitude in compliance with ITTC Procedures (2011, 20 times smaller). The length to height ratio is less than 3, so the grids sizes in the longitudinal direction also meet the ITTC requirements. Figure 4.6

illustrates the details of mesh configuration as well as grid size near the hull at the free surface. The prism layer mesh model is used with a core volume mesh to generate orthogonal prismatic cells next to wall surfaces and boundaries. Ten layers of such cells are defined to improve the accuracy of the flow solution. (Figure 4.6). For cases where there are large separations close to the body, such as the water free surface, K-ε and K- ω are the most commonly used turbulence models (Rodi, 1991, Wilcox, 1993, Shih et al., 1995, Arribas, 2007, Field and Wayne, 2013, Tezdogan et al., 2014b). The Shear-Stress Transport (SST) Menter K-ω and Realizable K-ε models are comparatively applied to determine the most effective CFD model in this specific case. More details regarding the characteristics and advantages of each of the CFD models in the current paper are further explained in Section 2.3.1. Considering the complexity of the problem and the similarity of the results, the Realizable K-ε model was chosen as the most effective turbulence model.

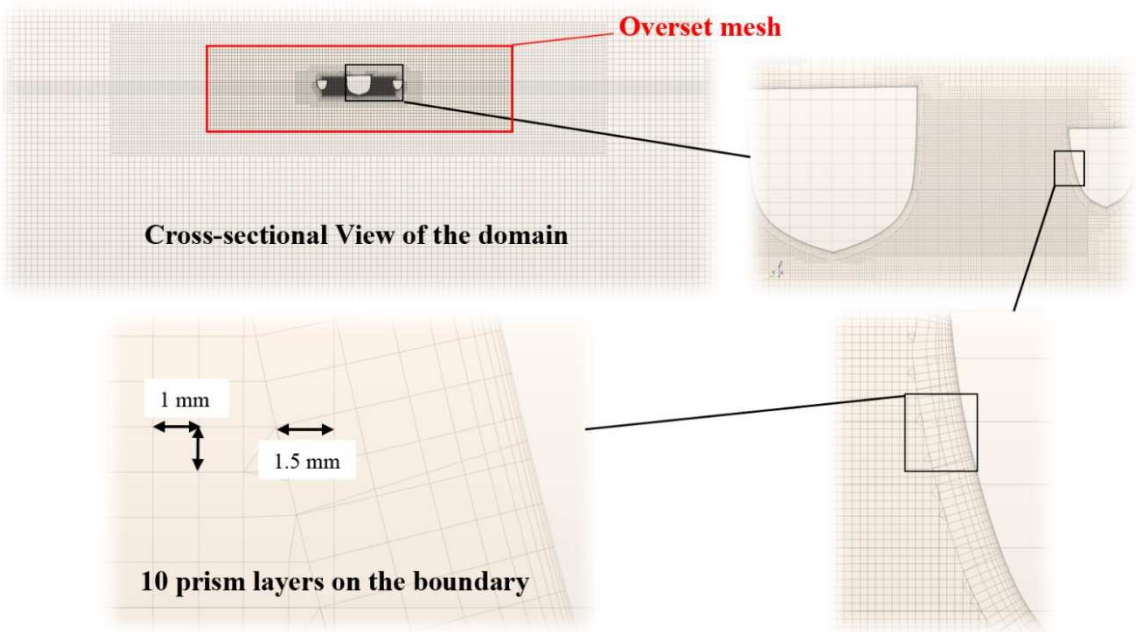

Figure 4.6 Cross-sectional view of the gridding system in Star CCM+ showing mesh cell sizes close to the free surface and the hull.

Uncertainty analysis was carried out based on the method of Stern et al. (2001). The numerical uncertainty (U_{SN}) consists of the iterative convergence uncertainty (U_I), the grid-spacing uncertainty (U_G), the time-step uncertainty (U_T) and Physical model uncertainty (U_P). Since U_I *and* U_P *were negligible in this case,* the grid-spacing and time step uncertainty calculations were performed based on a Richardson extrapolation (Jin et al., 2016), and following the outcomes, a fine mesh configuration with an efficient time step was chosen for the CFD model. Further details are given in Section 2.3.2. in Chapter 2

One of the underlying reasons behind the motion variation in different sea conditions is the wave interaction between the three hulls of the trimaran. According to computational results, the wave pattern of the main hull varies with speed. Figure 4.7 demonstrates the comparative influence of speed on the wave pattern and the interference between wave from the main hull and the waves generated by the outriggers at Froude numbers of Fr=0.3 and Fr=0.5 at wave frequencies of ω_e^*= 2.67 and ω_e^*= 3 at a constant wave heading of 160.9°. At Fr=0.3 (equivalent speed of 1.19 m/s), both areas A and B are affected by the main hull and outrigger hull wave

interference with the peak water surface elevation can be identified at about 0.055 m. For Fr=0.5 (equivalent speed of 1.98 m/s) areas A and B are hardly affected by the wave interaction of the main hull and outriggers, and the water surface elevation is about 0.03 m. It is evident that there has been a reduction in wave generation as well as water elevation at the higher speed. The wave interaction between the main hull and outriggers was seen to be the cause for the variation in motions that was observed during the model experiments.

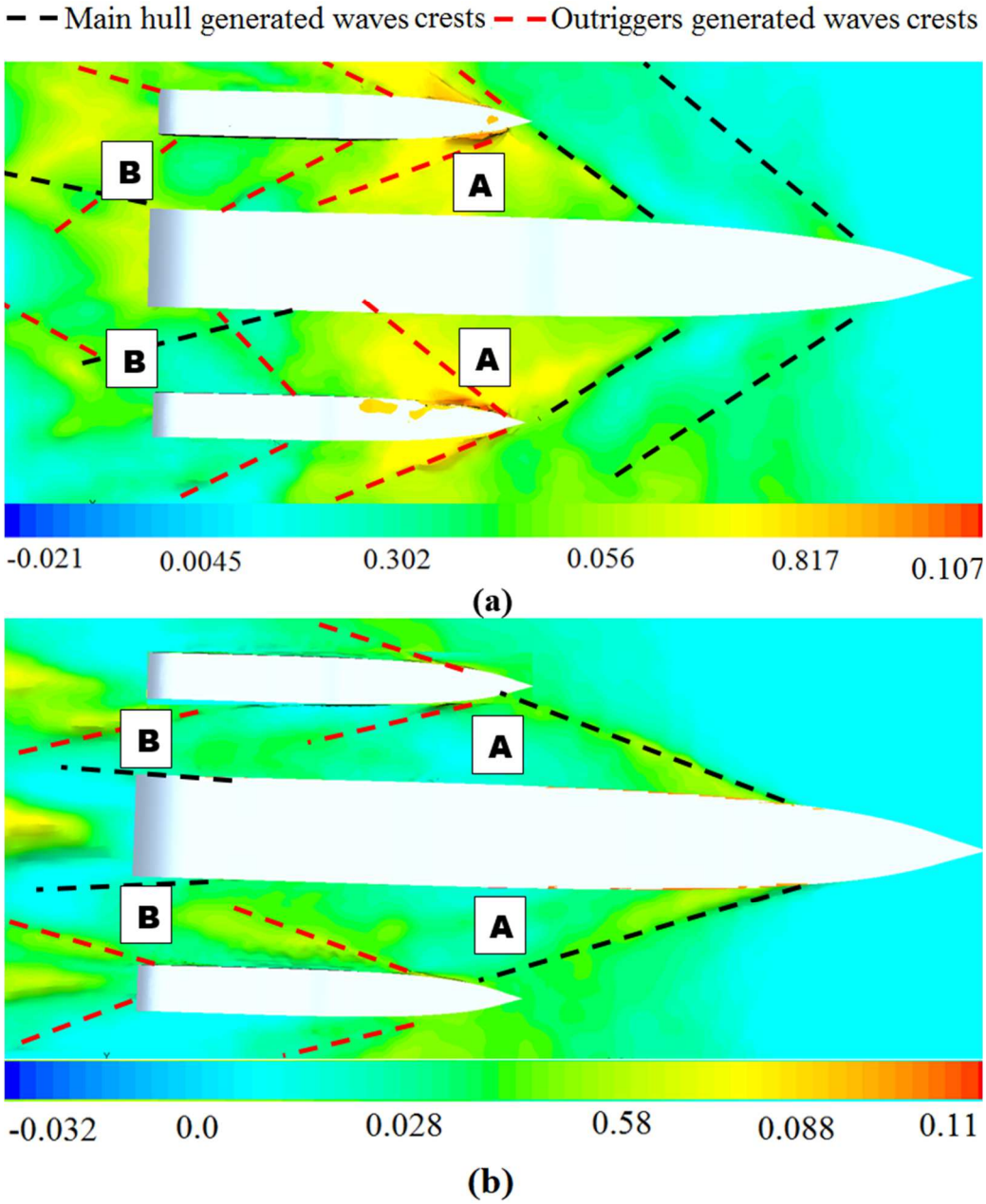

Figure 4.7 Water surface elevation (m) for (a) Fr= 0.3 (equivalent speed of 1.19 m/s) and dimensionless wave encounter frequency ω_e^*= 2.67. (b) Fr= 0.5 (equivalent speed of 1.98 m/s) and dimensionless wave encounter frequency ω_e^*= 3. The wave heading is 160.9°.

As can be seen in Figure 4.7, the complexity of the wave system between the main hull and outriggers at lower speeds (Fr=0.3) is greater than at the higher speed (Fr=0.5). Figure 4.8 shows the green water effect (i.e. water flow over the bow) on the deck of the main hull and outriggers at the speeds of 1.19 m/s, 1.59 m/s and 1.98 m/s (Fr=0.3, 0.4 and 0.5) and a range of wave frequencies (ω_e^*= 1.73-5.58). It was clearly seen from the

graphical CFD results that there is much greater water entry onto the deck of the main hull and outriggers at higher frequencies and at higher speed.

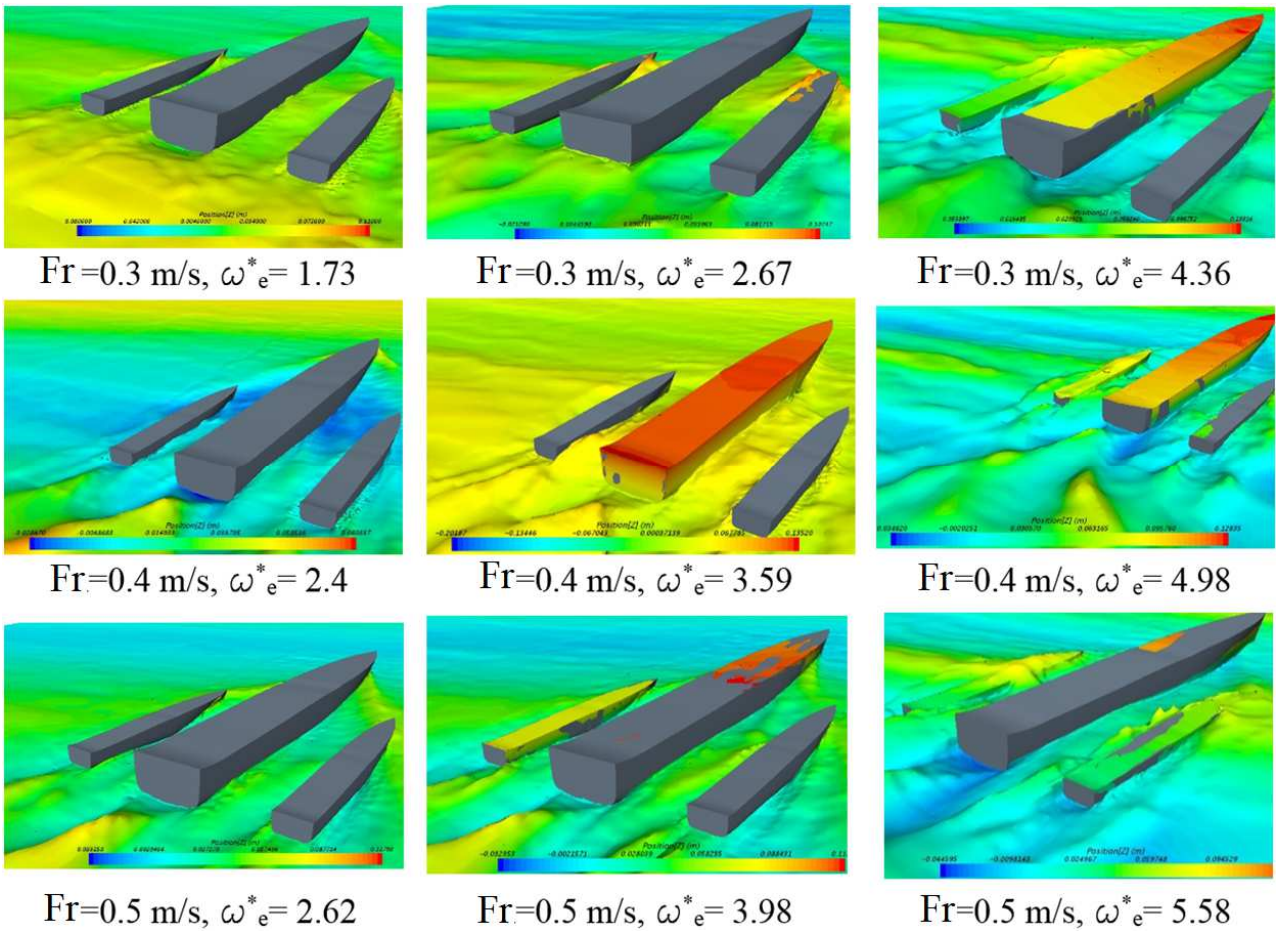

Figure 4.8 Green water visual representation from CFD results in 9 different conditions varying in Froude number from 0.3 to 0.5 and dimensionless wave encounter frequency ω_e^* of 1.73 to 5.58. The wave heading is 160.9°.

As can be observed, there is a rather complicated flow between the main hull and outriggers as shown by the CFD graphical results above. This complicated flow demonstrates the significant effect of the hull to hull interaction of the trimaran vessel and the importance of simulating this to determine the influence on motions both experimentally and numerically as has been the focus of the present study.

4.4 Comparison of CFD Results with Experimental Model Test Data

In Chapter 2, a validation process was performed for a CFD model to analyse the 1.6m trimaran in head waves. This CFD model has now been further extended to analyse the dynamic performance of the same trimaran model in oblique wave conditions. Here, the results of the CFD model are compared to the model test results.

Figures 4.9 to 4.12 show the heave, pitch and roll Response Amplitude Operators (RAOs) obtained for speeds of 1.981 m/s, 1.59 m/s and 1.19 m/s at a set wave height of 60 mm in regular oblique waves. The RAOs are plotted against dimensionless wave encounter frequency.

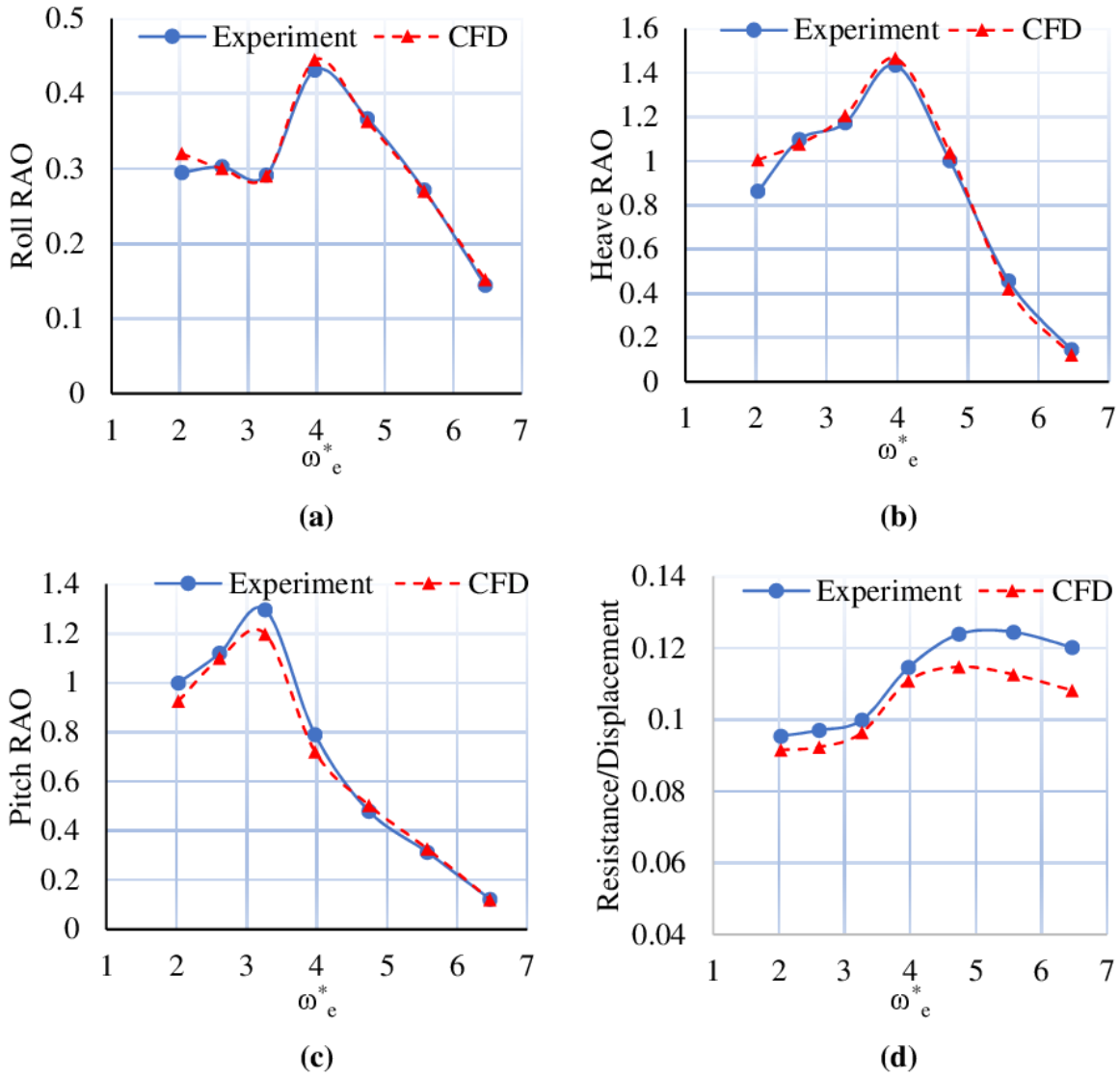

Figure 4.9 Comparison of CFD and experimental 1.6m trimaran model motion responses and added resistance in regular oblique seas at the higher model test speed of 1.98 m/s (Froude number = 0.5). wave heading 160.9º and wave height = 60 mm.

The trend of the CFD RAO plots computed by STAR-CCM+ for Froude number Fr=0.5 (equivalent forward speed of 1.98 m/s), appear to be consistent with the experimental results as shown in Figure 4.9. It is evident that the magnitude of the transfer function for roll (Figure 4.9a) starts at 0.325 (the Sine of the heading angle) at low frequency and reduces to small values (less than 0.2) at high wave encounter frequency as expected. We see that roll motion is not strong for these tests at a relatively small heading angle to the encountered sea and that there is a peak response of 0.45 at the dimensionless encounter frequency of ω_e^*= 4.1, which is close to the natural roll frequency. The heave peak response is 1.44 and occurs at the dimensionless encounter frequency of ω_e^*=4.1. The measured points obtained from experiment and CFD mostly coincide and thus provide a reliable validation of the CFD method as applied here except at the very low frequency of $\omega_e^* = 2$. In Figure 4.9c, the pitch transfer function has a peak at a frequency of $\omega_e^* = 3.3$ and reaches a peak at 1.3 in experiments. CFD computations compare well with the experimental measurements and capture the trend with minor differences at the peak. However, from Figure 4.9 (d) it can be seen that the CFD methods underestimate the added

resistance at higher frequencies when compared against experimental data. This could be due to dissimilarity in the set-up of the experiments and the CFD caused by the entry and escape of green water over the deck of the main hull and outriggers while moving at high speeds and encountering high frequency oblique waves. Green water entry was observed during the experiments so plastic sheets were installed at the bow (refer to right hand side photo in Figure 4.10) to prevent green water entering the main deck and draining overboard. Figure 4.10 shows a CFD generated diagram of the green water entering the main deck during simulation without the physical constraints (plastic sheets) installed during experiment. It is challenging to simulate the same condition precisely in the CFD model; thus, this is the likely discrepancy between the results of the two methods. However, the trend captured for the added resistance is similar in both measurements.

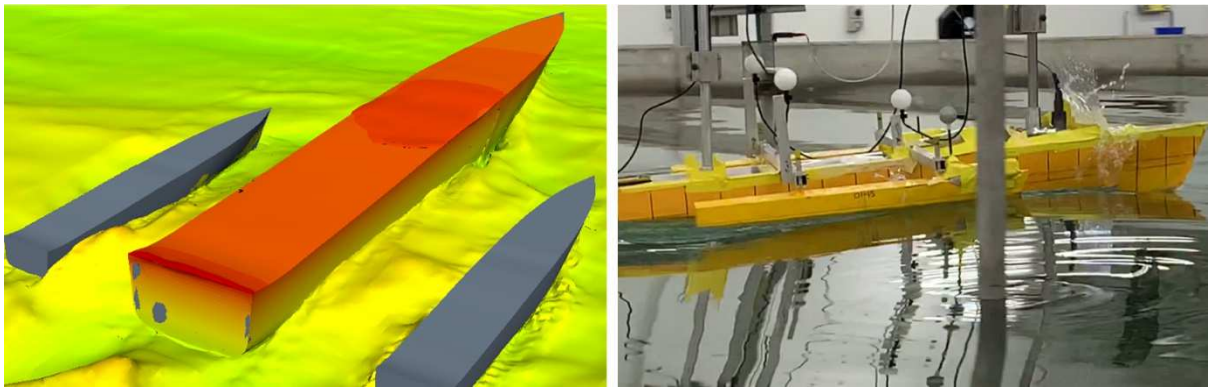

Figure 4.10 CFD and experimental model of the trimaran. Left hand side diagram shows entry and exit of green water during CFD simulation. Right hand side diagram shows plastic sheets that were used in experiments to prevent green water entry.

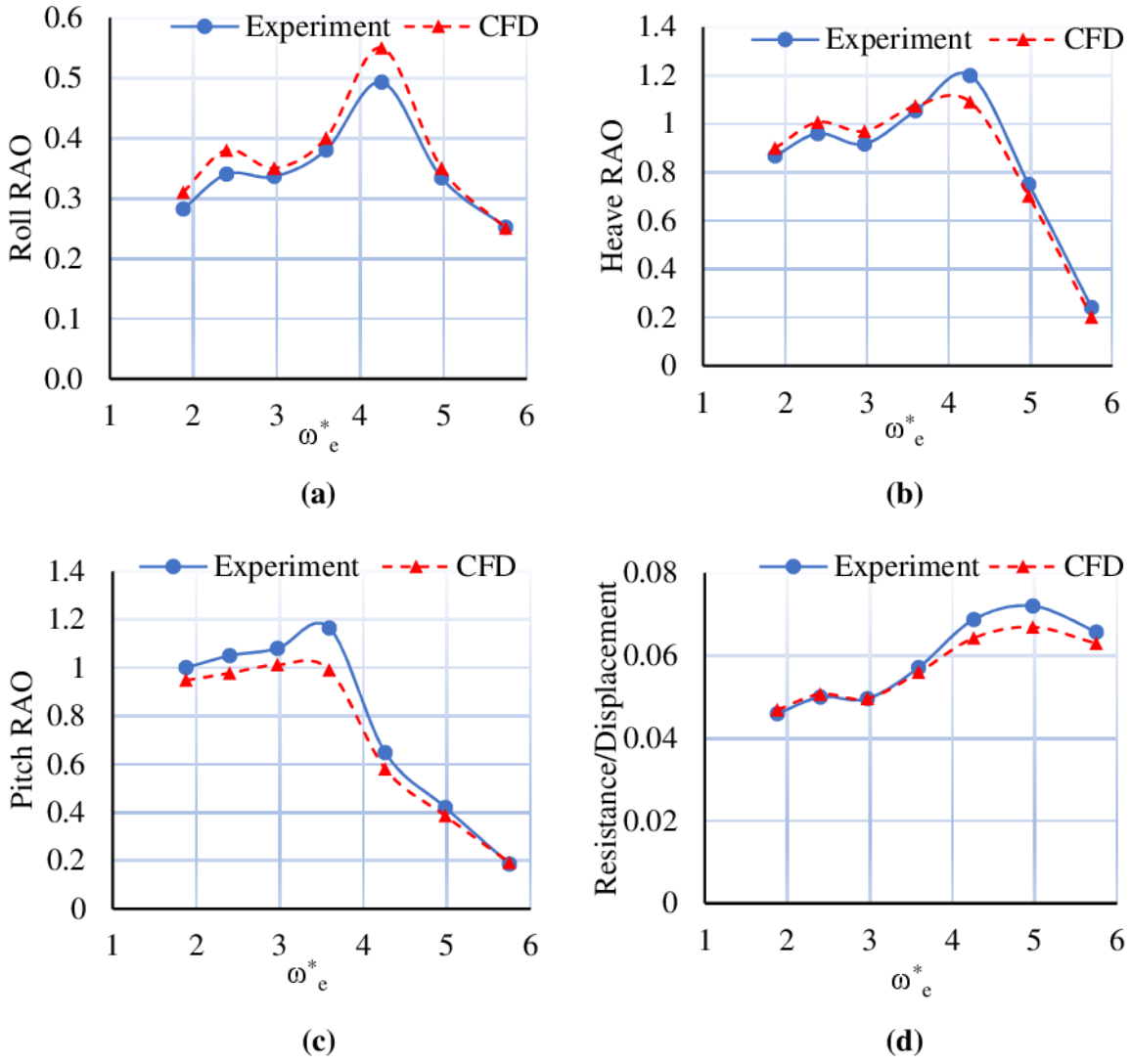

Figure 4.11 Comparison of CFD and experimental 1.6m trimaran model motion responses and added resistance in regular oblique seas at the model test speed of 1.59 m/s (Froude number = 0.4). wave heading 160.9º and wave height = 60 mm.

The results of CFD in comparison to experiments for a lower Froude number (V=1.59 m/s, Fr=0.4) is shown in Figure 4.11. The CFD results can be seen to be consistent with the experimental results shown in Figure 4.9. These CFD predictions have a slightly greater difference when compared with the experimental results than at the higher Froude number of Fr=0.5. As depicted in Figure 4.11a, the roll motions are not significant during this test condition and the RAO is once again about 0.325 at low frequency since the heading angle remains constant. Two peaks are detected in both CFD and experimental plots. The main peak is captured at close to the roll natural frequency and reaches 0.55 in magnitude. The second and less significant peak occurs at the lower frequency of ω_e^*=2.4. The second peak was not detected at Froude number of Fr=0.5, shown in Figure 4.9a. This is due to less wave interaction between the main hull and outriggers at higher speeds (Figure 4.7). In Figure 4.11b, the magnitude of the transfer function for heave starts at about 1 at low frequency, increases to a maximum of (1.2) at ω_e^*= (4.26) and declines more steeply at high wave encounter frequency. There are thus similarities to the roll RAO plot, where there is a peak response at ω_e^* =4.26 and a smaller peak at ω_e^*=2.4, which is also not observed at the higher Froude number (Figure 4.9b). It is evident that CFD overestimates the roll

magnitude by maximum of 11% at the peak response, but otherwise well predicts the heave motions with a difference of less than 8% when compared to experimental measurements. The pitch response, as shown in Figure 4.11c, has a similar trend to that shown in Figure 4.9c (Fr=0.5), but the CFD underestimates the pitch motions at lower frequencies and also at the frequency of maximum response. Although the maximum discrepancy is about 14%, the pitch response predicted by CFD more importantly does follow the same trend as the experimental test results. The added resistance prediction shown in Figure 4.11d is better than the prediction obtained at higher speed (Figure 4.9d), while CFD still tends to somewhat underestimate the magnitude at the peak frequency. This is due to a reduction in green sea on the decks but now at lower speed as described previously (Figure 4.8).

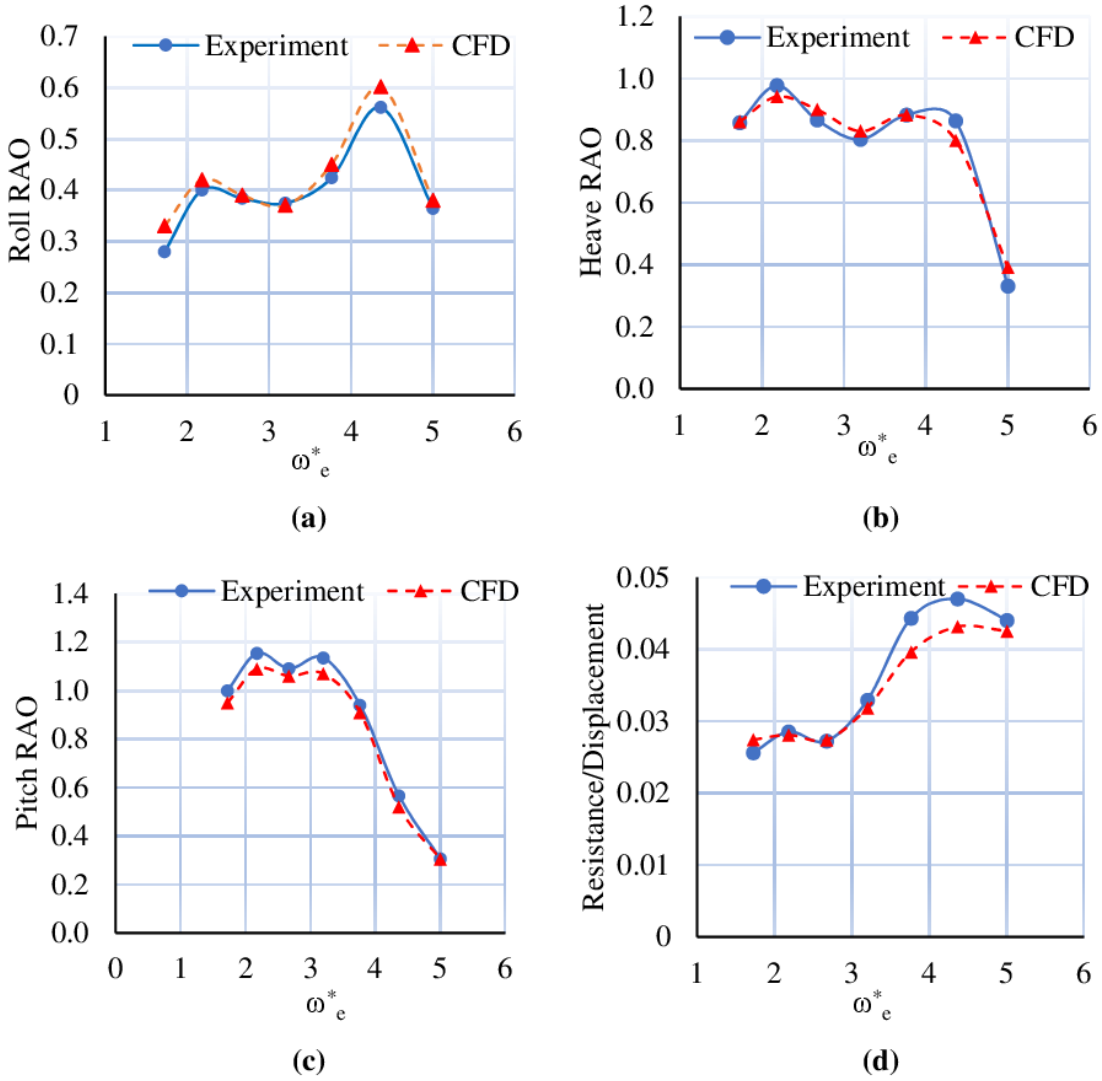

Figure 4.12 Comparison of CFD and experimental 1.6m trimaran model motion responses and added resistance in regular oblique seas at the lower model test speed of 1.19 m/s (Froude number = 0.3). wave heading 160.9° and wave height = 60 mm.

Figure 4.12 shows the motion responses and added resistance of the trimaran at speed of 1.19 m/s (Fr=0.3). The CFD computations compare relatively well with the experimental results for heave, pitch and roll motions whilst predicting the resonant peaks at ω_e^* = 2.2 and ω_e^* =4.3 more accurately. The CFD prediction underestimates the added resistance by less than 10% at frequencies between ω_e^*=3.7 and ω_e^*=5, where the

magnitude reaches its maximum. CFD prediction of roll motion at the frequency of maximum response has been improved when compared to the previous two cases (Fr=0.5 and Fr=0.4) and the discrepancy between CFD and experiments at that point is less than 7%. Two peaks are detected in all four plots. The first peak is recorded at the dimensionless wave frequency of ω_e^*=2.2 for all plots. This is due to the higher wave interaction effect at the lower Froude number of 0.3. The main peak in the roll and heave RAOs as well as added resistance plot is consistent with the roll natural frequency (ω_e^*=4.3) while a double peak occurs at ω_e^*=2.2 and ω_e^*=3.2 in the pitch response amplitude plot for both CFD and experiment.

Further to previous studies, it is expected that the reflected waves generated by the main hull and outriggers are more complicated at lower speeds. The findings show that CFD methods can be used to analyse the dynamic performance of multihull vessels and the results for roll motion amplitude at higher speeds are more reliable than at lower speeds. Further studies of wave deflection and wave interference between the main hull and outriggers are deemed necessary.

4.5 Conclusion

The experimental results obtained in this study demonstrate the effect of the changes of operating speed on the trimaran motion responses and resistance force. It is evident from the results that the speed has a significant impact on the trimaran motions in oblique regular seas. The study also set out to develop a CFD model for the prediction of trimaran model motions in oblique regular waves. The CFD model results were compared to the experimental tests carried out in the Model Test Basin.

Based on the comparison of the CFD simulations to experimental results, the trends of the RAO plots for the trimaran motions follow similar patterns for all speeds tested. Two peaks are observed in motion response amplitudes of the trimaran model at lower speeds. The development of these two peaks is mainly due to wave interaction effects between the main hull and outriggers, which reduces at higher speeds as was demonstrated by the CFD simulation. With regard to roll motion, the highest responses are developed at the lower speeds: this could be due to stronger wave interaction effects and a dynamic effect due to forward speed as a result of inertia about the roll axis. Roll and heave amplitude operators showed opposite trends with forward speed when encountering oblique sea directions. It was further observed that the main peak responses in roll and heave RAO were close to the natural roll frequency predicted for this specific trimaran. It was shown that increasing the operational speed can increase the heave response by two thirds and can reduce the roll response by a quarter, emphasising clearly the influences due to forward speed. The model speed affects the added resistance magnitude quite considerably, with increases in drag force in proportion to velocity squared as expected. The peaks of resistance to displacement ratio were also identified at dimensionless encounter frequencies coinciding closely with the dimensionless natural roll frequency for this type of hull form.

CFD computations have been shown to compare relatively well with the experimental results, satisfactorily predicting the peaks. The computations and measurements have less differences at a higher Froude number of Fr=0.5. However, added resistance prediction, is more accurate at lower Froude numbers. This may be due to green water entry and exit on the deck of main hull and outriggers during higher speed at specific wave encounter frequencies. Overall, the CFD somewhat overestimates the roll responses and underestimates the pitch responses

and resistance forces. Whilst a range of 10%-14% discrepancy in frequencies of maximum response was found, the CFD methods appear to deliver reliable data in predicting both motions and added resistance of trimarans while more importantly showing similar trends with experimental test results.

The findings highlight the importance of operational condition on the dynamic performance of trimarans for this specific hull type as well as the effect of wave interference in prediction methods when undergoing variations in oblique wave encounter. The developed CFD model can be further extended to better understand the response of the trimaran model under more varied test conditions. In particular the results of this investigation can form the basis for further analysis of trimaran motions to investigate parameter sensitivities according to wave condition, vessel speed, size and configuration of outriggers and weight distribution of the vessel. This leading to establishing a more systematic basis for effective design of trimaran vessels in the future. In particular, it would now be valuable to investigate by CFD the effect pf trimaran design parameters on rolling and pitching at greater heading angles than was possible in the experimental tests carried out here.

Chapter 5: Conclusions

5.1 Summary

Trimarans are innovative hull-form concepts that combine advantages of both catamaran and mono-hull vessels, such as having large deck areas and slender hulls which provide low wave making resistance and low added resistance in high seas. Having a slender main hull and larger deck area, their dynamic stability is largely dependent on the positioning of the outriggers. Therefore, studying different configurations and analysing the main sources of trimaran motions is crucial, including wave interference between the main hull and outriggers in the primary stages of conceptual design. This research has developed a better understanding of the influential factors on the motions and added resistance of such vessels using experimental and computational approaches.

A 1.6 m trimaran model from AME CRC systematic series was chosen to be analysed computationally using Computational Fluid Dynamics (CFD). In particular, the capability of CFD methods in solving RANS equations for a high-speed trimaran vessel in head waves was investigated. Therefore, a series of simulations were conducted by a CFD based commercial unsteady RANS solver, Star CCM+. Gridding system and time step analysis were performed, and different turbulence models were investigated. The outcomes were compared against existing numerical results using linear Strip Theory and the results obtained from experimental model test data in head-seas. In order to validate the primary CFD method, the Response Amplitude Operators (RAOs) of the trimaran motions are compared against the two sets of previously conducted experimental data obtained from the tests on the same trimaran model in regular head waves at Australian Maritime College Towing Tank.

On completion of the head-seas analysis, a set of experimental tests were conducted for eight different configurations of the physical trimaran model in oblique waves. The tests were primarily utilised as a basis for studying the effect of different parameters on heave, pitch and roll motions as well as added resistance of a trimaran model in oblique wave test conditions. Subsequently, this set of data was used to validate the previously developed head-seas CFD model to investigate the effect of the oblique sea test conditions. This enabled the further verification of the CFD model that can now be further used for analysing the effect of a broad range of parameters influencing the dynamic performance of trimarans.

The motions RAOs were determined for two stagger ratios (*ST,* longitudinal position of outriggers), two separation ratios (*CL,* Transverse position of outriggers) and two buoyancy fractions (*B*, Vertical position of outriggers) of outriggers at three different speeds of 1.19, 1.59 and 1.98 m/s (equivalent Froude numbers of 0.3, 0.4 and 0.5) while undertaking various wave conditions.

The major outcomes of the thesis are categorised based on the methodology and briefly explained in the next two sections. Based on the outcomes of this thesis, a set of recommendations for extended future studies are included to form the final section of this thesis.

5.2 Major outcomes of experimental study

Significant findings emerged from the parametric experimental study of the trimaran dynamic performance in regular oblique waves. The results demonstrate considerable impact of the location of outriggers on the trimaran motion responses and the resultant added resistance force when moving at different speeds while undertaking oblique sea wave encounter. The most surprising aspect of the data is the two peaks identified in motion RAOs of the trimaran, which is different from those of monohull ships. It was found that the secondary peak is due to the impact of wave interaction between three hulls of the trimaran.

Observations made during the tests in oblique seas show appearance of green water on the deck of both main hull and outriggers, which suggest slight discrepancy between CFD and experiment. It was found that the position of the outriggers, hull shape above the waterline, speed, wave frequency, wave height and buoyancy fraction of outriggers will determine the magnitude of the dynamic phenomenon (Motion response and added resistance of the trimaran) and its impact on the performance of the trimaran undergoing different sea conditions.

It was found that the wave interaction between the main hull and outriggers has a large impact on the motion response of the trimaran when operating in oblique waves. The response heavily depends on the position of the outriggers, wave characteristics including (wave height, frequency and heading), the ratio of the width of the hull to the width of the hull spacing and the operational speed. It was also found that wave interaction effects between the main hull and outriggers is more significant in the narrower configuration of outriggers. It is evident from the results that with an increase in Stagger ratio (*ST,* longitudinal spacing of main and demi-hulls transoms/overall length), Separation ratio (*CL*, separation of outrigger centre lines/overall length) and Buoyancy fraction of outriggers (*B, %*), the roll motion is reduced, heave motion and added resistance are increased, and pitch motions are slightly influenced.

It was evident that the roll motions could vary by as much as a factor of five between Configuration #2 (*ST=0,* longitudinal spacing of main and demi-hulls transoms/overall length), Separation ratio (*CL=0.4*, separation of outrigger centre lines/overall length) and Buoyancy fraction of outriggers (*B=7 %*) and configuration #6 (*ST=0.2,* longitudinal spacing of main and demi-hulls transoms/overall length), Separation ratio (*CL=0.5*, separation of outrigger centre lines/overall length) and Buoyancy fraction of outriggers (*B=16 %*), and the variation for the heave motions and added resistance is considerable between different configurations. Heave response of the trimaran in oblique sea is less significant than those recorded in head seas and is mostly affected by the longitudinal position than transverse position of outriggers. The variation in pitch response is more directly linked with the variation in RoG_{Pitch} of the waterplane area and it is otherwise only slightly affected by the variation in arrangement of outriggers. However, configurations with less buoyancy fraction (Configurations #1, #2, #7 and #8) show slightly higher peak value of pitch response. The added resistance magnitude can vary by up to 20% in different outriggers configurations. By comparison, the higher the stagger ratio, the higher will be the detected variation in added resistance amplitude. However, variation in *CL* has the least effect on added resistance. Nevertheless, added resistance significantly increases when the buoyancy fraction increases, as might be expected due to increased immersion of the outriggers. These findings suggest that minimising the roll amplitude by optimising the configuration may cause an increase in the hull

added resistance, and therefore a compromise should be maintained between motion and added resistance when designing a trimaran. For instance, Configuration #2 (Minimum stagger ratio, separation ratio and buoyancy fraction of outriggers) has a minimum added resistance magnitude and maximum roll response among other configurations.

The findings also suggest that in configurations with higher stagger ratios where the roll motion is considerably reduced, the added resistance increases, which is due to the increase in wave making resistance. These Configurations, however, give the maximum heave response peaks.

It was found that, where the waterplane area of outriggers remains unchanged, the longitudinal position of outriggers has substantial effect on the roll response at the higher buoyancy fractions. It was also concluded that when longitudinally located in the forward position, the outrigger buoyancy fraction has more effect on the roll response than their transverse position, and once increased, reduces the roll motions. However, the opposite is true when the outriggers are in the aft position.

The results also suggest that motion responses and added resistance of the trimaran model are sensitive to speed variation. The roll and heave peak responses for all speeds fall in the proximity of the natural roll frequency, and there are considerable differences between the peak responses at different speeds.

The trimaran roll, heave and pitch RAO responses generally have two peaks, which are mainly due to the wave interaction effects between the main hull and outriggers. At higher speeds (Fr=0.5), where there is less wave interference between the three bodies, the roll and heave response amplitudes show only one main peak. The findings also suggest that highest roll responses are developed in lower speeds (Fr=0.3). The pitch motion is not affected by the variation of speed as much as observed in the roll and heave RAO plots. It was evident that the model speed affects the resistance magnitude considerably and the variation seems to be proportionate to the square of speed (V^2).

In terms of increasing the operational speed from 1.19 m/s (Fr=0.3) to 1.98 m/s (Fr=0.5), the heave response increases by two third and the roll response reduces by a quarter. The ratio of wave encounter frequency to the natural roll frequency plays a big role in the wave interference between the hulls, and hence the motion response of the trimaran. Where this value is closer to 1, the resonant occurs.

5.3 Major outcomes of CFD modelling

The findings suggest that Computational Fluid Dynamic (CFD) methods are more efficient than linear strip theory based (STF) methods in prediction of trimaran motion responses while taking in to account the green seas, hull shape above waterline and breaking waves. The recorded variations are up to 14% when compared to experimental model test results. Green seas and wave deformation in CFD are identified as main sources of discrepancy in calculations due to wave-current-wind interaction. The SST Menter K ω turbulence model proved a more accurate turbulence model than Realizable K-ε, while the hull shape above waterline is taken into consideration. Using this turbulence model, the wave interference between the main hull and outriggers is captured.

The assumption of linearity in using STF methods neglects the effect of variations in the hull form above and below the waterline, which makes the motion results less consistent with the experiments. Moreover, STF methods fail to capture the maximum pitch RAO at the frequency of maximum normalised response in head seas.

The CFD model that was initially developed improved the predicted motions response for a semi displacement trimaran moving at speeds of 1.19 m/s and 1.98 m/s (Fr=0.3 and Fr=0.5) undergoing regular head waves (Wave amplitude of 20 mm). The results are in better agreement with the experiments for heave and pitch motion for normalised amplitudes showing trends similar to the towing tank tests. However, in some cases, the calculated motion response is slightly different than the measured experimental value. This seems mostly to happen at the frequencies of maximum response, between ω_e^*= 3.4 and ω_e^*= 4.4.

The simulation outcomes of the improved CFD model developed for oblique seas are in good agreement with model test data in most conditions. At higher speeds the green seas effect on deck increases, where there is less wave interference between the main hull and outriggers. Therefore, at higher speeds, better motion predictions but limited added resistance predictions are resulted.

When comparing the results of the motions responses, there is less discrepancy between the computations and measurements in higher Froude numbers. However, in the case of added resistance prediction, it is vice versa, and prediction seems more accurate in lower Froude numbers. The main reason is due to extreme water splash on the deck of main hull and outriggers in higher speed at some encounter frequencies.

Furthermore, CFD detects the asymmetric conditions of the wave perturbation forces and moments acting on each hull. That is when the forces acting on an outrigger towards the incoming wave is larger than the forces induced on the outrigger away due to the reduction of wave energy as the wave encounters three hulls successively.

Overall, CFD well predicts the heave responses, slightly overestimates the roll responses and underestimates the pitch responses and resistance forces of the trimaran undergoing different oblique wave encounters. Showing 10%-14% discrepancy in limited frequencies of maximum responses (almost equal to natural roll frequency, ω_e^*= 4.4) , CFD methods appear to deliver reliable results in predicting both motions and added resistance of trimarans at the speed range of 1.19 m/s and 1.98 m/s (Fr=0.3 and Fr=0.5) whilst showing similar trends recorded with experimental test in MTB.

5.4 Recommendations for future work

The findings of this thesis highlight the importance of investigating trimarans outrigger arrangement for further understanding of their dynamic performance in oblique wave encounter scenarios. However, there is still a need to develop a better understanding of the parameters that influence trimaran motions, in particular roll motions. The limitations of the current investigation were on the wave heading angle as well as other geometric variations (different hull geometries with different C_M, C_{WP}, etc) both in experiments and CFD studies, where this work must proceed is by undertaking further experiments at greater oblique angles and then simulating those conditions (both wave headings and geometries) in CFD to further validate the CFD methods. In doing so

one should then be able to identify the environment/geometric conditions that exposes trimarans to extreme roll motions. An important case study of this is the roll motions of Condor Liberation, the Austal trimaran the extreme roll motion of which was shown at the start of this thesis. It is how the results obtained in this thesis can lead the way forward in addressing this problem. This could help establish a more systematic basis for effective design of trimaran vessels in the future. Upon developing confidence in the numerical techniques adopted here, it is now proposed to extend the experiments and the computations for further contribution in the body of knowledge. The proposed research opportunities include but are not limited to:

- Analysing the effect of broader wave heading angles on the motions and added resistance of trimarans in regular waves with experimental and numerical approaches.
- Further CFD and experimental investigation on the effect of position of outriggers on the performance of trimaran vessels.
- Measuring and calculating motion velocity and acceleration of different geometries of the trimaran in order to create the capability of assessing the passenger discomfort in different outriggers configurations.
- Investigation of different shapes of main hull, outriggers and cross-sections.
- Conducting a case study of the motions of a trimaran (e.g. Condor Liberation) in different oblique wave conditions.

References

1. ADYGIL. 2008. Earthrace [Online]. [Accessed 2019].
2. API 2000. Recommended practice for planning, designing and constructing fixed offshore platforms. working stress design.
3. Armstrong, T. & Holden, K. 2003. A new generation of large fast ferry-from concept to contract reality. FAST 2003, 75-84. Ischia, Italia.
4. ARRIBAS, F. P. 2007. Some methods to obtain the added resistance of a ship advancing in waves. Ocean Engineering, 34**,** 946-955.
5. AUSTAL-SHIPS. 2019. Benchijigua [Online]. [Accessed 2020].
6. Banks, M. & Abdussamie, N. 2017. The response of a semisubmersible model under focused wave groups: Experimental investigation. Journal of Ocean Engineering and Science, 2**,** 161-171.
7. Bhattacharyya R. 1978. Dynamics of marine vehicles New York: Ocean engineering, Wiley series.
8. Beck, R., Reed, A., Sclavounos, P. & Hutchison, B. 2001. Modern computational methods for ships in a seaway. Discussion. Author's closure. Transactions-Society of Naval Architects and Marine Engineers, 109**,** 1-51.
9. BERTRAM, V. & SEIF, M. New developments for fast and unconventional marine vehicles. 4th International Conference on High Performance Marine Vehicles, Rome, 2004. 28-43.
10. Bingham A, Hampshire J, Miao S, Temarel P. Motions and loads for a trimaran travelling in regular waves. Proceedings of the Proceedings of 6th International Conference on Fast Sea Transportation (FAST2001); 2001: Royal Institution of Naval Architects.
11. Boote, D., Colaianni, T. & Pino, E. Seakeeping analysis of a trimaran fast ferry. 4th International Conference of High-Performance Marine Vehicle (HIPER), 304-316., 2004. 304-316.
12. CD-ADAPCO 2017. User guide, STAR-CCM+. Star-CCM+.
13. CMN-GROUP. 2016. Ocean Eagle 43 [Online]. [Accessed 2019].
14. Date, J. C. & Turnock, S. R. 1999. A Study into the Techniques Needed to Accurately Predict Skin Friction Using RANS Solvers with Validation Against Froude's Historical Flat Plate Experimental Data. Ship Science Report. Southampton, UK: University of Southampton.
15. Dean R G, Dalrymple R. A. 1991. Water Wave Mechanics for Engineers and Scientists: World Scientific Publishing Company.
16. De Luca, F., S. Mancini, S. Miranda, e C. Pensa. «An Extended Verification and Validation Study of CFD Simulations for Planing Hulls. *Journal of Ship Research* in press (2016).
17. De Marco, Agostino, Simone Mancini, Salvatore Miranda, Raffaele Scognamiglio, e Luigi Vitiello. «Experimental and Numerical Hydrodynamic Analysis of a Stepped Planing Hull. *Applied Ocean Research* (Elsevier) 64 (2017): 135-154.
18. Dingemans MW. 1997. Water wave propagation over uneven bottoms. NASA Sti/Recon Technical Report N, Advanced series on Ocean engineering.
19. Dobashi, J. 2014. On the prediction method for ship motions of trimaran in oblique waves. Journal of the Japan Society of Naval Architects and Ocean Engineers, 20**,** 77-84.
20. Doctors, L. Application of the boundary-element method to bodies oscillating near a free surface. International Symposium on Computational Fluid Dynamics ISCFD, 1:377-386, August 24-27, 1988 Sydney, Australia. 377-386.

21. Doctors, L. 1993. HYDROS: integrated software for the analysis of the hydrostatics and hydrodynamics of marine vehicles. 10th international Maritime and Shipping Symposium (Ship Shape 2000), 1:373-392. The University of New South Wales, Australia.
22. Doctors, L. & Scrace, R. The optimization of trimaran side hull position for minimum resistance. Seventh International Conference on Fast Transportation (FAST 2003), October 2003 Ischia, Italy. 1-12.
23. Doctors, L. J. 2015. Hydrodynamics of high-performance marine vessels, Vol 2. Charleston, SC: CreateSpace Independent Publishing Platform, 2015. ISBN: 978151489430; PP:247.
24. Lin Du, Hamid Hefazi & Prasanta Sahoo (2019) Rapid resistance estimation method of non-Wigley trimarans, Ships and Offshore Structures, 14:8, 910-920, DOI: 10.1080/17445302.2019.1588499
25. ELECTRIC, B. 2014. MV Brigitte Bardot [Online]. [Accessed 2019].
26. Enshaei H., S. S. K. 2018. Quantifying Ship's Dynamic Stability through Numerical Investigation of Weight Distribution. Proceedings of the 13th Int. Conference on the Stability of Ships and Ocean Vehicles (STAB 2018), 16-21 September 2018, Kobe, Japan.
27. FACH, K. 2004. Classification aspects of HSC multihulls. 4th International Conference on High-Performance Marine Vehicle (HIPER), 317-322.
28. Faltinsen, O., Landarini, M. & Lugni, C. Hydrodynamic Aspects of High-Speed Vessels. Proc. 7th International Conference on Fast Sea Transportation, 1:13-22, 2003. 13-22.
29. Faltinsen, O. & Zhao, R. 1991. Numerical predictions of ship motions at high forward speed. Phil. Trans. R. Soc. Lond. A, 334**,** 241-252.
30. FANG, M. C. & TOO, G. Y. 2006. The effect of side hull arrangements on the motions of the trimaran ship in waves. Naval engineers journal, 118**,** 27-37.
31. Field, P. L. & Wayne, L. N. Comparison of RANS and Potential Flow Force Computations for the ONR umble home Hull form in Vertical Plane Radiation and Diffraction Problems. ASME 2013 32nd International Conference on Ocean, Offshore and Arctic Engineering, June 9–14, 2013 2013. Virginia Polytechnic Institute and State University, Blacksburg, VA., 23.
32. Ghadimi, P., Nazemian, A. & Ghadimi, A. 2019. Numerical scrutiny of the influence of side hulls arrangement on the motion of a Trimaran vessel in regular waves through CFD analysis. Journal of the Brazilian Society of Mechanical Sciences and Engineering, 41**,** 1.
33. Grafton, T. J. 2007. The roll motion of trimaran ships. Doctor of Philosophy, University College London.
34. Hebblewhite, K., Sahoo, P. K. & Doctors, L. 2007. A case study: theoretical and experimental analysis of motion characteristics of a trimaran hull form. Ships and Offshore Structures, 2**,** 149-156.
35. Hirdaris S, Temarel P. 2009. Hydroelasticity of ships: recent advances and future trends. Proceedings of the Institution of Mechanical Engineers, Part M: Journal of Engineering for the Maritime Environment.223:305-330.
36. ITTC Procedures. 2011. Guidelines. 2011. In: Practical Guidelines for Ship CFD Applications: ITTC.
37. JERSEY ACTION GROUP 2016. Temporary Ferry Tenerife is shaken violently by the waves in Los Cristianos. https://www.youtube.com/watch?v=Yi4iU0a56-M. Jersey Action Group (accessed 07th July 2017)
38. JIANG, S. C., BAI, W. & TANG, G. Q. 2018. Numerical simulation of wave resonance in the narrow gap between two non-identical boxes. Ocean Engineering, 156**,** 38-60.
39. JIN, Y., Chai, S., Duffy, J., Chin, C., Bose, N. & Templeton, C. 2016. RANS prediction of FLNG-LNG hydrodynamic interactions in steady current. Applied Ocean Research, 60**,** 141-154.

40. JT901 2015. Condor Liberation rough crossing Poole to Jersey high seas. In: YOUTUBE (ed.) https://www.youtube.com/watch?v=Gf3QwpOkovs. (Accessed 07th July 2017)
41. KIANEJAD, S., ENSHAEI, H., DUFFY, J. & ANSARIFARD, N. 2019. Prediction of a ship roll added mass moment of inertia using numerical simulation. Ocean Engineering, 173**,** 77-89.
42. KIM, M.-G., Jung, K.-H., Park, S.-B., LEE, G.-N., Park, I.-R. & SUH, S.-B. 2019. Study on Roll Motion Characteristics of a Rectangular Floating Structure in Regular Waves. Journal of Ocean Engineering and Technology, 33**,** 131-138.
43. KIM, S.-Y., KIM, K.-M., PARK, J.-C., JEON, G.-M. & CHUN, H.-H. 2016. Numerical simulation of wave and current interaction with a fixed offshore substructure. International Journal of naval Architecture and ocean engineering, 8**,** 188-197.
44. Lindstrom, J., Sirvio, J. & YLI-RANTALA, A. Superslender monohull with outriggers, 1:295. 1995 Lubek Travemunde, Germany. 295.
45. Lloyd A. 1989. Seakeeping: ship behaviour in rough weather.
46. Lloyd A. 1998. Seakeeping Ship behaviour in Rough Weather. ARJM Lloyd, 26 Spithead Avenue, Gosport. Hampshire, United Kingdom.
47. MAKI, K., DOCTORS, L., SCHER, R., WILSON, W., RHEE, S., TROESCH, A. & BECK, R. 2009. Conceptual design and hydrodynamic analysis of a high-speed sealift adjustable-length trimaran. Trans.-Soc. Nav. Archit. Mar. Eng., 116, 16-39.
48. MENTER, F. R. 1994. Two-equation eddy-viscosity turbulence models for engineering applications. AIAA journal, 32**,** 1598-1605.
49. Molin, B., Remy, F., Camhi, A. & Ledoux, A. Experimental and numerical study of the gap resonances in-between two rectangular barges. 13th congress of international maritime association of mediterranean, 2009.
50. Molland AF. 2011. The maritime engineering reference book: a guide to ship design, construction and operation: Elsevier.
51. Moolman, R. 2005. Comparative evaluation of a hydrofoil-assisted trimaran. Master's degree, Stellenbosch: University of Stellenbosch.
52. Nakayama, Y. 2018. Introduction to fluid mechanics, Butterworth-Heinemann.
53. Newman, J. N. 1979. The theory of ship motions. Advances in applied mechanics. Elsevier.
54. NIGELIRENS. 1998. Cable and Wireless adventurer [Online]. [Accessed].
55. Nowruzi, L., Enshaei, H., Lavroff, J. & Davis, M. R. 2020a. Parametric study of seakeeping of a trimaran in regular oblique waves. Ships and Offshore Structures, 1-12.
56. Nowruzi, L., Enshaei, H., Lavroff, J., Kianejad, S. S. & Davis, M. R. Motions and added resistance of a high-speed trimaran in regular oblique waves. International Conference on Ships and Offshore Structures, ICSOS 2019, Florida, USA, November 4-8, 2019 Florida, USA.
57. Nowruzi, L and Enshaei, H and Lavroff, J and Kianejad, SS and Davis, MR, CFD simulation of motion responses of a trimaran in regular head waves, Royal Institution of Naval Architects (RINA) Transactions. Part A1. International Journal of Maritime Engineering, 162, (Part A1) pp. 91-106. ISSN 1479-8751 (2020b).

58. Oberkampf, W. L., e F. G. Blottner. Issues in Computational Fluid Dynamics Code Verification and Validation. AIAA Journal 5, n. 36 (May 1998): 687-695.
59. ONAS, A. S. 2009. Nonlinear roll motions of a frigate-type trimaran and susceptibility to parametric roll resonance. Doctor of Philosophy thesis, Stevens Institute of Technology.
60. Pattison D, Zhang J. Trimaran ships. Proceedings of the RINA Spring Meetings Paper; 1994.
61. RODI, W., 1991, January. Experience with two-layer models combining the k-epsilon model with a one-equation model near the wall. In *29th Aerospace sciences meeting*, 1991. p. 216.
62. SALVESEN, N., TUCK, E. & FALTINSEN, O. 1970. Ship motions and sea loads. Trans. SNAME, 78**,** 250-287.
63. SEN, D. 2016. Time domain simulation of side-by-side floating bodies using a 3D numerical wave tank approach. Applied Ocean Research, 58**,** 189-217.
64. SHIH, T.-H., LIOU, W.-W., SHABBIR, A., YANG, Z. & ZHU, J. 1995. A new k-ϵ eddy viscosity model for high Reynolds number turbulent flows. Computers & Fluids, 24**,** 227-238.
65. SIMONSEN, C. D., OTZEN, J. F., JONCQUEZ, S. & STERN, F. 2013. EFD and CFD for KCS heaving and pitching in regular head waves. Journal of Marine Science and Technology, 18**,** 435-459.
66. Smith, R. P. & Jones, J. B. 2001. Design, construction and trials of the trident trimaran test craft. Jahrbuch Schiffbau Technische Gesellschaft, 355-362, 355-362.
67. STERN, F., WILSON, R. & SHAO, J. 2006. Quantitative V&V of CFD simulations and certification of CFD codes. International journal for numerical methods in fluids, 50**,** 1335-1355.
68. STERN, F., WILSON, R. V., COLEMAN, H. W. & PATERSON, E. G. 2001. Comprehensive approach to verification and validation of CFD simulations-Part 1: methodology and procedures. Transactions-American Society of Mechanical Engineers Journal of Fluids Engineering, 123**,** 793-802.
69. SUN, L., TAYLOR, R. E. & TAYLOR, P. H. 2010. First-and second-order analysis of resonant waves between adjacent barges. Journal of Fluids and Structures, 26**,** 954-978.
70. TAN, L., TANG, G.-Q., ZHOU, Z.-B., CHENG, L., CHEN, X. & LU, L. 2017. Theoretical and numerical investigations of wave resonance between two floating bodies in close proximity. Journal of Hydrodynamics, 29**,** 805-816.
71. TEZDOGAN, T., DEMIREL, Y. K., INCECIK, A. & TURAN, O. 2014b. Hydrodynamics of heaving twin cylinders in a free surface using an unsteady-RANS method. The 2nd International Conference on Maritime Technology (ICMT2014).
72. TEZDOGAN, T., INCECIK, A. & TURAN, O. 2014a. Operability assessment of high-speed passenger ships based on human comfort criteria. Ocean Engineering, 89**,** 32-52.
73. Wang S, Ma S, Duan W. 2018. Seakeeping optimization of trimaran outrigger layout based on NSGA-II. Applied Ocean Research.78:110-122.
74. WANG, X.-L., HU, J.-J., GU, X.-K., GENG, Y.-C. & XU, C. 2011. Comparative Studies of the Transverse Structure Design Wave Loads for a Trimaran by Model Tests and Rule Calculations [J]. Journal of Ship Mechanics, p. 3.
75. Wikipedia 2018. Trimaran. Wikipedia. http://en.wikipedia.org/wiki/Trimaran.
76. Wilcox DC. 1993. Turbulence modelling for CFD: DCW industries La Canada, CA.

77. Wu C-s, Zhou D-c, Gao L, Miao Q-m. 2011. CFD computation of ship motions and added resistance for a high-speed trimaran in regular head waves. International journal of naval architecture and ocean engineering.3:105-110.
78. Yasukawa H. 2005. Influence of Outrigger Position on the Performances of a High-Speed Trimaran, Japan Society of Naval Architects and Ocean Engineers, 189-195.
79. Yun L, Bliault A, Rong HZ. 2018. High Speed Catamarans and Multihulls: Technology, Performance, and Applications: Springer.